

# New Results on $B \rightarrow \pi, K, \eta$ Decay Formfactors from Light-Cone Sum Rules

PATRICIA BALL<sup>\*,1</sup> AND ROMAN ZWICKY<sup>†,2</sup>

<sup>1</sup> IPPP, Department of Physics, University of Durham, Durham DH1 3LE, UK

<sup>2</sup> William I. Fine Theoretical Physics Institute,  
University of Minnesota, Minneapolis, MN 55455, USA

## Abstract:

We present an improved calculation of  $B \rightarrow$  light pseudoscalar formfactors from light-cone sum rules, including one-loop radiative corrections to twist-2 and twist-3 contributions, and leading order twist-4 corrections. The total theoretical uncertainty of our results at zero momentum transfer is 10 to 13% and can be improved, at least in part, by reducing the uncertainty of hadronic input parameters, in particular those describing the twist-2 distribution amplitudes of the  $\pi$ ,  $K$  and  $\eta$ . We present our results in a way which details the dependence of the formfactors on these parameters and facilitates the incorporation of future updates of their values from e.g. lattice calculations.

*Submitted to Physical Review D*

---

\*Patricia.Ball@durham.ac.uk

†zwick@physics.umn.edu

# 1 Introduction

This paper aims to give a new and more precise determination of the decay formfactors of  $B$  mesons into light pseudoscalar mesons, i.e.  $\pi$ ,  $K$  and  $\eta$ . We do not include the  $\eta'$  which is too heavy to be treated in this framework. The calculation uses the method of QCD sum rules on the light-cone, which in the past has been rather successfully applied to various problems in heavy-meson physics, cf. Refs. [1, 2, 3, 4, 5]<sup>1</sup>; an outline of the method will be given below. Our calculation improves on our previous papers [3, 4] by

- including radiative corrections to twist-3 contributions to one-loop accuracy, for all formfactors;
- a precisely defined method for fixing the sum rule specific parameters;
- using updated values for input parameters;
- a careful analysis of the uncertainties of the formfactors at zero momentum transfer;
- a new parametrization of the dependence of the formfactors on momentum transfer, which is consistent with the constraints from analyticity and heavy-quark expansion;
- detailing the dependence of formfactors on nonperturbative hadronic parameters describing the  $\pi$ ,  $K$ ,  $\eta$  mesons, the so-called Gegenbauer moments, which facilitates the incorporation of future updates of their numerical values and also allows a consistent treatment of their effect on nonleptonic decays treated in QCD factorisation.

The motivation for this study is twofold and related to the overall aim of  $B$  physics to provide precision determinations of quark flavor mixing parameters in the Standard Model. Quark flavor mixing is governed by the unitary CKM matrix which depends on four parameters: three angles and one phase. The constraints from unitarity can be visualized by the so-called unitarity triangles (UT); the one that is relevant for  $B$  physics is under intense experimental study. The over-determination of the sides and angles of this triangle from a multitude of processes will answer the question whether there is new physics in flavor-changing processes and where it manifests itself. One of the sides of the UT is given by the ratio of CKM matrix elements  $|V_{ub}/V_{cb}|$ .  $|V_{cb}|$  is known to about 2% accuracy from both inclusive and exclusive  $b \rightarrow c\ell\nu$  transitions [7], whereas the present error on  $|V_{ub}|$  is much larger and around 15%. Its reduction requires an improvement of experimental statistics, which is under way at the  $B$  factories BaBar and Belle, but also and in particular an improvement of the theoretical prediction for associated semileptonic spectra and decay rates. This is the first motivation for our study of the  $B \rightarrow \pi$  decay formfactor  $f_+^{B \rightarrow \pi}$ , which, in conjunction with alternative calculations, in particular from lattice [8], will help to reduce the uncertainty from exclusive semileptonic determinations of  $|V_{ub}|$ . Secondly, formfactors of general  $B \rightarrow \text{light meson}$  transitions are also needed as ingredients in the analysis of nonleptonic two-body  $B$  decays, e.g.  $B \rightarrow K\pi$ , in the framework of QCD factorization [9], again with the objective to extract CKM parameters. One issue calling for particular attention in this context is the effect of SU(3) breaking, which enters both the formfactors and the  $K$  and  $\eta$  meson distribution amplitudes figuring

---

<sup>1</sup>See also Ref. [6] for reviews.

in the factorization analysis. We would like to stress here that the implementation of SU(3) breaking in the light-cone sum rules approach to formfactors is *precisely* the same as in QCD factorization and is encoded in the difference between  $\pi$ ,  $K$  and  $\eta$  distribution amplitudes, so that the use of formfactors calculated from light-cone sum rules together with the corresponding meson distribution amplitudes in factorization formulas allows a unified and controlled approach to the assessment of SU(3) breaking effects in nonleptonic  $B$  decays.

As we shall detail below, QCD sum rules on the light-cone allow the calculation of formfactors in a kinematic regime where the final state meson has large energy in the rest-system of the decaying  $B$ ,  $E \gg \Lambda_{\text{QCD}}$ . This is in contrast to lattice calculations which presently are available only for  $B \rightarrow \pi$  and  $q^2 > 15 \text{ GeV}^2$ , due to the restriction to  $\pi$  energies smaller than the inverse lattice spacing.<sup>2</sup> First unquenched results are underway [10, 11], which, once published, will allow one to exploit the complementarity of lattice simulations and light-cone sum rules in more detail.

The physics underlying  $B$  decays into light mesons at large momentum transfer can be understood qualitatively in the framework of hard exclusive QCD processes, pioneered by Brodsky and Lepage et al. [12]. The hard scale in  $B$  decays is  $m_b$  and one can show that to leading order in  $1/m_b$  the decay is described by two different parton configurations: one where all quarks have large momenta and the momentum transfer happens via the exchange of a hard gluon, the so-called hard-gluon exchange, and a second one where one quark is soft and does interact with the other partons only via soft-gluon exchange, the so-called soft or Feynman-mechanism. The consistent treatment of both effects in a framework based on factorization, i.e. the clean separation of perturbatively calculable hard contributions from nonperturbative “wave functions”, is highly nontrivial and has spurred the development of SCET, an effective field theory which aims to separate the two relevant large mass scales  $m_b$  and  $\sqrt{m_b \Lambda_{\text{QCD}}}$  in a systematic way [13]. In this approach formfactors can indeed be split into a calculable factorizable part which roughly corresponds to the hard-gluon exchange contributions, and a nonfactorizable one, which includes the soft contributions and cannot be calculated within the SCET framework [14]. Predictions obtained in this approach then typically aim to eliminate the soft part and take the form of relations between two or more formfactors whose difference is expressed in terms of factorizable contributions.

The above discussion highlights the need for a calculational method that allows numerical predictions while treating both hard and soft contributions on the same footing. It is precisely QCD sum rules on the light-cone (LCSRs) that accomplish this task. LCSRs can be viewed as an extension of the original method of QCD sum rules devised by Shifman, Vainshtein and Zakharov (SVZ) [15], which was designed to determine properties of ground-state hadrons at zero or low momentum transfer, to the regime of large momentum transfer. QCD sum rules combine the concepts of operator product expansion, dispersive representations of correlation functions and quark-hadron duality in an ingenious way that allows the calculation of the properties of non-excited hadron-states with a very reasonable theoretical uncertainty. In the context of weak-decay formfac-

---

<sup>2</sup>This situation may change in the future with the successful implementation of “moving NRQCD” [10], where the  $B$  decays while moving “backwards”, which gives access to smaller values of  $q^2$  without increasing the discretisation error.

tors, the basic quantity is the correlation function of the weak current and a current with the quantum numbers of the  $B$  meson, evaluated between the vacuum and a light meson. For large (negative) virtualities of these currents, the correlation function is, in coordinate-space, dominated by distances close to the light-cone and can be discussed in the framework of light-cone expansion. In contrast to the short-distance expansion employed by conventional QCD sum rules à la SVZ where nonperturbative effects are encoded in vacuum expectation values of local operators with vacuum quantum numbers, the condensates, LCSRs rely on the factorization of the underlying correlation function into genuinely nonperturbative and universal hadron distribution amplitudes (DAs)  $\phi$  which are convoluted with process-dependent amplitudes  $T$ . The latter are the analogues of the Wilson-coefficients in the short-distance expansion and can be calculated in perturbation theory. The light-cone expansion then reads, schematically:

$$\text{correlation function} \sim \sum_n T^{(n)} \otimes \phi^{(n)}. \quad (1)$$

The sum runs over contributions with increasing twist, labelled by  $n$ , which are suppressed by increasing powers of, roughly speaking, the virtualities of the involved currents. The same correlation function can, on the other hand, be written as a dispersion-relation, in the virtuality of the current coupling to the  $B$  meson. Equating dispersion-representation and the light-cone expansion, and separating the  $B$  meson contribution from that of higher one- and multi-particle states using quark-hadron duality, one obtains a relation for the formfactor describing the decay  $B \rightarrow \text{light meson}$ .

Our paper is organized as follows: in Sec. 2 we define all relevant quantities, in particular correlation functions and meson distribution amplitudes. In Sec. 3 we outline our calculations and derive the light-cone sum rules. In Sec. 4 we present our numerical results and Sec. 5 contains a summary and conclusions. Detailed expressions for distribution amplitudes and explicit formulas for the light-cone sum rules are given in the appendices.

## 2 Definitions

The formfactors  $f_+^P$ ,  $f_0^P$  and  $f_T^P$  which are relevant for the  $B \rightarrow P$  transition, where  $P$  stands for  $\pi$ ,  $K$  or  $\eta$ , are defined as follows:<sup>3</sup>

$$\langle P(p) | V_\mu^P | B(p_B) \rangle = \left\{ (p + p_B)_\mu - \frac{m_B^2 - m_P^2}{q^2} q_\mu \right\} f_+^P(q^2) + \left\{ \frac{m_B^2 - m_P^2}{q^2} q_\mu \right\} f_0^P(q^2), \quad (2)$$

$$\langle P(p) | J_\mu^{P,\sigma} | B(p_B) \rangle = \frac{i}{m_B + m_P} \left\{ q^2 (p + p_B)_\mu - (m_B^2 - m_P^2) q_\mu \right\} f_T^P(q^2, \mu), \quad (3)$$

where  $V_\mu^{\pi,\eta} = \bar{u}\gamma_\mu b$  is the standard weak current,  $V_\mu^K$  is given by  $V_\mu^K = \bar{s}\gamma_\mu b$  and  $J_\mu^{\pi(\eta),\sigma} = \bar{d}\sigma_{\mu\nu}q^\nu b$ ,  $J_\mu^{K,\sigma} = \bar{s}\sigma_{\mu\nu}q^\nu b$  are penguin currents. The momentum transfer is given by  $q = p_B - p$  and the physical range in  $q^2$  is  $0 \leq q^2 \leq (m_B - m_P)^2$ . The formfactors  $f_+^P$  and  $f_0^P$  are independent of the renormalization scale  $\mu$  since  $V_\mu$  is a physical current, in contrast to the penguin current  $J_\mu^\sigma$ . Note that  $f_+^P(0) = f_0^P(0)$  which is a consequence of

---

<sup>3</sup>The following notations are frequently used in the literature:  $f_+ = F_1$  and  $f_0 = F_0$ .

the parametrization chosen in Eq. (2). We assume SU(2) isospin symmetry throughout this work, i.e. we do not distinguish  $\bar{B}^0 \rightarrow \pi^+$  and  $B^- \rightarrow \pi^0$  formfactors etc.

In the semileptonic decay  $B \rightarrow \pi l \nu_l$  the formfactor  $f_0^\pi$  enters proportional to the lepton mass  $m_l^2$  and hence is irrelevant for light leptons ( $l = e, \mu$ ), where only  $f_+^\pi$  matters. The semileptonic decay can be used to determine the size of the CKM matrix element  $|V_{ub}|$  from the spectrum

$$\frac{d\Gamma}{dq^2}(B \rightarrow \pi l \nu_l) = \frac{G_F^2 |V_{ub}|^2}{192 \pi^3 m_B^3} \lambda(q^2)^{3/2} |f_+^\pi(q^2)|^2, \quad (4)$$

where  $\lambda(x) = (x + m_B^2 - m_\pi^2)^2 - 4m_B^2 m_\pi^2$ . The formfactor  $f_0^\pi$  will be relevant in and can be measured from the decay  $B \rightarrow \pi \tau \nu_\tau$ .  $f_T^\pi$  is relevant for the rare decay  $B \rightarrow \pi l^+ l^-$ , where the penguin current features in the effective Hamiltonian of the process.

Our starting point for calculating the formfactors  $f_{+,0}^\pi$  is the correlation function

$$\begin{aligned} \Pi_\mu(q, p_B) &= i \int d^4x e^{iq \cdot y} \langle \pi(p) | T V_\mu(x) j_B^\dagger(0) | 0 \rangle \\ &= \Pi_+(q^2, p_B^2)(p + p_B)_\mu + \Pi_-(q^2, p_B^2)q_\mu, \end{aligned} \quad (5)$$

where  $j_B = m_b \bar{d} i \gamma_5 b$  is the interpolating field for the  $B$  meson. For the calculation of  $f_T^\pi$ ,  $V_\mu$  has to be replaced by  $J_\mu^\sigma$ . For virtualities

$$m_b^2 - p_B^2 \geq O(\Lambda_{\text{QCD}} m_b), \quad m_b^2 - q^2 \geq O(\Lambda_{\text{QCD}} m_b), \quad (6)$$

the correlation function (5) is dominated by light-like distances and therefore accessible to an expansion around the light-cone. The above conditions can be understood by demanding that the exponential factor in (5) vary only slowly. The light-cone expansion is performed by integrating out the transverse and “minus” degrees of freedom and leaving only the longitudinal momenta of the partons as relevant degrees of freedom. The integration over transverse momenta is done up to a cutoff,  $\mu_{\text{IR}}$ , all momenta below which are included in a so-called hadron distribution amplitude  $\phi$ , whereas larger transverse momenta are calculated in perturbation theory. The correlation function is hence decomposed, or factorized, in perturbative contributions  $T$  and nonperturbative contributions  $\phi$ , which both depend on the longitudinal parton momenta and the factorization scale  $\mu_{\text{IR}}$ . If the  $\pi$  is an effective quark-antiquark bound state, as is the case to leading order in the light-cone expansion, we can write the corresponding longitudinal momenta as  $up$  and  $(1-u)p$ ,  $p$  being the momentum of the  $\pi$ . The schematic relation (1) can then be written in more explicit form as

$$\Pi_+(q^2, p_B^2) = \sum_n \int_0^1 du T^{(n)}(u, q^2, p_B^2, \mu_{\text{IR}}) \phi^{(n)}(u, \mu_{\text{IR}}). \quad (7)$$

As  $\Pi_+$  itself is independent of the arbitrary scale  $\mu_{\text{IR}}$ , the scale-dependence of  $T^{(n)}$  and  $\phi^{(n)}$  must cancel each other.<sup>4</sup> If  $\phi^{(n)}$  describes the meson in a two-parton state, it is called

---

<sup>4</sup>If there are more than one contributions of a given twist, they will mix under a change of the factorization scale  $\mu_{\text{IR}}$  and it is only in the sum of all such contributions that the residual  $\mu_{\text{IR}}$  dependence cancels.

a two-particle distribution amplitude (DA), if it describes a three-parton, i.e. quark-antiquark-gluon state, it is called three-particle DA. In the latter case the integration over  $u$  gets replaced by an integration over two independent momentum fractions, say  $\alpha_1$  and  $\alpha_2$ . Eq. (7) is called a “collinear” factorization formula, as the momenta of the partons in the  $\pi$  are collinear with the  $\pi$ ’s momentum, and its validity actually has to be verified. We will come back to that issue in the next section.

Let us now define the distribution amplitudes to be used in this paper. Again we only quote formulas for the  $\pi$  meson, those for the  $K$  and  $\eta$  are analogous. All definitions and formulas are well-known and can be found in Ref. [16]. In general, the distribution amplitudes we are interested in are related to nonlocal matrix elements of type

$$\langle 0 | \bar{u}(x) \Gamma[x, -x] d(-x) | \pi(p) \rangle \quad \text{or} \quad \langle 0 | \bar{u}(x) [x, vx] \Gamma G_{\mu\nu}^a(vx) \lambda^a / 2 [vx, -x] d(-x) | \pi(p) \rangle.$$

$x$  is light-like or close to light-like and the light-cone expansion is an expansion in  $x^2$ ;  $v$  is a number between 0 and 1 and  $\Gamma$  a combination of Dirac matrices. The expressions  $[x, -x]$  etc. denote Wilson lines that are needed to render the matrix elements, and hence the DAs, gauge-invariant. One usually works in the convenient Fock-Schwinger gauge  $x^\mu A_\mu^a(x) \lambda^a / 2 = 0$ , where all Wilson lines are just **1**; we will suppress them from now on. The DAs are ordered by twist, i.e. the difference between spin and dimension of the corresponding operators. We will include DAs of twist-2 (the leading twist), 3 and 4. The leading-twist DA  $\phi_\pi$  is defined as

$$\begin{aligned} \langle 0 | \bar{u}(x) \gamma_\mu \gamma_5 d(-x) | \pi^-(p) \rangle &= i f_\pi p_\mu \int_0^1 du e^{i\zeta p \cdot x} \left[ \phi_\pi(u) + \frac{1}{4} m_\pi^2 x^2 \mathbb{A}(u) \right] \\ &+ i f_\pi \frac{m_\pi^2}{p x} x_\mu \int_0^1 du e^{i\zeta p \cdot x} g_\pi(u) + O(x_\mu x^2) \end{aligned} \quad (8)$$

with  $\zeta \equiv 2u - 1$  and  $p^2 = 0$ . The above matrix element also contains two twist-4 DAs,  $g_\pi$  and  $\mathbb{A}$ . The variable  $u$  can be interpreted as the momentum fraction carried by the quark (as opposed to the antiquark) in the meson.

There are two two-particle twist-3 DAs,  $\phi_p$  and  $\phi_\sigma$ , which are defined as

$$\langle 0 | \bar{u}(x) i \gamma_5 d(-x) | \pi(p) \rangle = \mu_\pi^2 \int_0^1 du e^{i\zeta p \cdot x} \phi_p(u), \quad (9)$$

$$\langle 0 | \bar{u}(x) i \sigma_{\mu\nu} \gamma_5 d(-x) | \pi(p) \rangle = -\frac{i}{3} \mu_\pi^2 (1 - \rho_\pi^2) (p_\mu x_\nu - x_\mu p_\nu) \int_0^1 du e^{i\zeta p \cdot x} \phi_\sigma(u), \quad (10)$$

where  $\mu_\pi^2 \equiv f_\pi m_\pi^2 / (m_u + m_d)$  and  $\rho_\pi^2 \equiv (m_u + m_d)^2 / m_\pi^2$ .

The precise definitions of three-particle DAs are a bit cumbersome and given in App. B. The salient feature is that there is one three-particle DA of twist-3 and four of twist-4.

Although we have introduced not less than 10 different DAs, which are all nonperturbative quantities, it may seem, at first glance, that light-cone sum rules do not retain much predictive power. Fortunately, however, it turns out that the DAs are highly constrained functions which can be analysed in the framework of conformal expansion, a topic being discussed in App. B. The main result is that, to next-to-leading order in

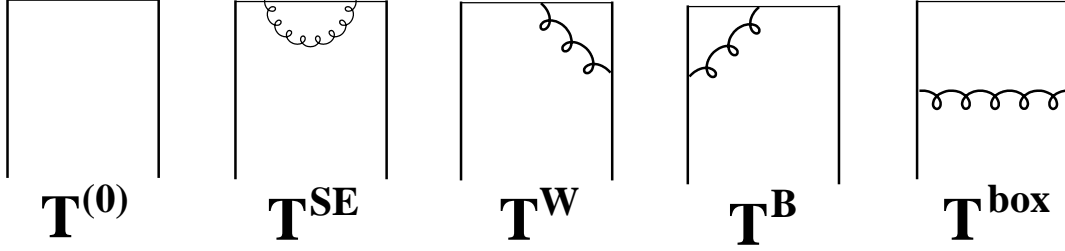


Figure 1: Perturbative contributions to the correlation function  $\Pi$ . The external quarks are on-shell with momenta  $up$  and  $(1-u)p$ , respectively.

conformal expansion, which is sufficient for the accuracy we are aiming at, all 10 DAs can be expressed in terms of 7 independent hadronic parameters.

This completes the definitions necessary for the calculation of formfactors.

### 3 The Sum Rules

The diagrams to be calculated to  $O(\alpha_s)$  for two-particle DAs are shown in Fig. 1. The quark (antiquark) is collinear with the light meson and carries momentum  $up$  ( $(1-u)p$ ). Quarks are projected onto the corresponding distribution amplitudes using the completeness relation

$$\begin{aligned} \bar{u}_a d_b &= \frac{1}{4} (\mathbf{1})_{ba} (\bar{u}d) - \frac{1}{4} (i\gamma_5)_{ba} (\bar{u}i\gamma_5 d) + \frac{1}{4} (\gamma_\mu)_{ba} (\bar{u}\gamma^\mu d) - \frac{1}{4} (\gamma_\mu\gamma_5)_{ba} (\bar{u}\gamma^\mu\gamma_5 d) \\ &+ \underbrace{\frac{1}{8} (\sigma_{\mu\nu})_{ba} (\bar{u}\sigma^{\mu\nu} d)}_{\equiv -\frac{1}{8} (\sigma_{\mu\nu}i\gamma_5)_{ba} (\bar{u}\sigma^{\mu\nu}i\gamma_5 d)} . \end{aligned}$$

The diagrams are calculated in momentum space. The terms in  $x_\mu$  in the contribution of  $\phi_\sigma$ , Eq. (10), are rewritten in terms of derivatives

$$x_\mu \rightarrow -i \frac{\partial}{\partial (up)_\mu}.$$

In the previous section we mentioned that the fact that  $\Pi$  can be written in factorized form can not be taken for granted, but requires proof. We do not attempt to give a proof to all orders in  $\alpha_s$ , although that should be possible using the techniques of SCET, but restrict ourselves to  $O(\alpha_s)$  in twist-2, to all orders in the conformal expansion, and to  $O(\alpha_s)$  and leading order in the conformal expansion for twist-3. The proof essentially relies on the cancellation of singularities, of which there are several possible types: infrared and ultraviolet singularities arising from loop calculations and so-called soft singularities which occur when the integral over  $u$  in Eq. (7) does diverge at the endpoints. The latter divergences have actually posed a severe problem in early attempts to treat  $f_+^\pi$  in QCD factorization: in Ref. [17] only the hard gluon exchange was included, which yields a logarithmic divergence for the parton configuration where the  $u$  quark emerging from the



weak decay carries essentially all pion momentum. As we understand now, this divergence disappears when contributions from the Feynman-mechanism are added. In our case, it turns out that all  $T$  are regular at the endpoints  $u = 0, 1$ , so there are *no soft divergences, independent of the end-point behavior of the distribution amplitudes*. As for infrared and ultraviolet singularities, they can be treated in dimensional regularisation. Using the lowest-order expression of the Brodsky-Lepage evolution kernel for  $\phi_\pi$  derived in [12], we have followed the strategy outlined in [18] to check that the infrared divergences precisely cancel those contained in the bare DA  $\phi_\pi^{\text{bare}}$ . As for twist-3, the evolution kernel is not known, so we have only checked the cancellation of infrared divergences of the lowest order term in the conformal expansion, whose divergent behavior is well known – in fact, only the one-loop renormalisation of the quark condensate is needed. The ultraviolet divergences cancel for  $f_+$  and  $f_0$ , which are physical formfactors and hence do not depend on the ultraviolet renormalisation scale; for  $f_T$ , we reproduce the well-known one-loop anomalous dimension.

We then have used the explicit expressions for the twist-2 and 3 two-particle DAs given in App. B to perform the integration over  $u$  analytically. Actually it is not the correlation function  $\Pi$  itself that is needed, but its imaginary part, see below.  $\Pi$  has a cut in  $p_B^2$  starting at  $m_b^2$  and taking the imaginary part after integration over  $u$  is straightforward. The strategy outlined here is different from the procedure we followed in our previous papers [3, 4], where we took the imaginary part before integrating over  $u$ . This latter procedure resulted in expressions with a very complicated analytical structure which made it impossible to give explicit formulas for the imaginary parts. With our new procedure we obtain lengthy, but not very complicated expressions; the complete set of spectral densities  $\rho = (\text{Im } \Pi)/\pi$  for the sum rule for the formfactor  $f_+$  is given in App. C.

Armed with the spectral densities, we can derive the LCSR for e.g. the formfactor  $f_+$ . The basic quantity is  $\Pi_+$ , which is calculated in two ways. In light-cone expansion, it can be written in dispersive representation as

$$\Pi_+^{\text{LC}}(p_B^2, q^2) = \int_{m_b^2}^{\infty} ds \frac{\rho_+^{\text{LC}}(s, q^2)}{s - p_B^2} \quad (11)$$

with the explicit expression for the spectral density  $\rho_+^{\text{LC}}(s)$  given in App. C. This expression has to be compared to the physical correlation function, which also features a cut in  $p_B^2$ , starting at  $m_B^2$ :

$$\Pi_+^{\text{phys}}(p_B^2, q^2) = \int_{m_B^2}^{\infty} ds \frac{\rho_+^{\text{phys}}(s, q^2)}{s - p_B^2}; \quad (12)$$

the spectral density is given by hadronic contributions and reads

$$\rho_+^{\text{phys}}(s, q^2) = f_B m_B^2 f_+(q^2) \delta(s - m_B^2) + \rho_+^{\text{higher-mass states}}(s, q^2). \quad (13)$$

Here  $f_B$  is the  $B$  meson decay constant defined as

$$\langle 0 | \bar{q} \gamma_\mu \gamma_5 b | B \rangle = i f_B p_\mu \quad \text{or} \quad (m_b + m_q) \langle 0 | \bar{q} i \gamma_5 b | B \rangle = m_B^2 f_B. \quad (14)$$

To obtain a light-cone sum rule for  $f_+$ , one equates the two expressions for  $\Pi_+$  and uses quark-hadron duality to approximate

$$\rho_+^{\text{higher-mass states}}(s, q^2) \approx \rho_+^{\text{LC}}(s, q^2) \Theta(s - s_0), \quad (15)$$



where  $s_0$ , the so-called continuum threshold is a parameter to be determined within the sum rule approach itself. In principle one could now write a sum rule

$$\Pi_+^{\text{phys}}(p_B^2, q^2) = \Pi_+^{\text{LC}}(p_B^2, q^2)$$

and determine  $f_+$  from it. However, in order to suppress the impact of the approximation (15), one subjects both sides of the equation to a Borel transformation

$$\frac{1}{s - p_B^2} \rightarrow \hat{B} \frac{1}{s - p_B^2} = \frac{1}{M^2} \exp(-s/M^2)$$

which ensures that contributions from higher-mass states be sufficiently suppressed and improves the convergence of the OPE. We then obtain

$$e^{-m_B^2/M^2} m_B^2 f_B f_+(q^2) = \int_{m_b^2}^{s_0} ds e^{-s/M^2} \rho_+^{\text{LC}}(s, q^2). \quad (16)$$

This is the final sum rule for  $f_+$ ; expressions for the other formfactors are obtained analogously. The task now is to find sets of parameters  $M^2$  (the Borel parameter) and  $s_0$  (the continuum threshold) such that the resulting formfactor does not depend too much on the precise values of these parameters; in addition the continuum contribution, that is the part of the dispersive integral from  $s_0$  to  $\infty$  that has been subtracted from both sides of (16), should not be too large, say less than 30% of the total dispersive integral.

## 4 Numerics

In this section we obtain numerical results from the sum rules (16). The section is organised as follows: in Sec. 4.1 we explain how we determine the sum rule specific parameters, i.e. the Borel parameter  $M^2$  and the continuum threshold  $s_0$ . We also determine  $f_B$ , which is a necessary ingredient in (16). In Sec. 4.2 we explain in more detail how we fix the hadronic input parameters, in particular the Gegenbauer moments  $a_{1,2,4}$  that describe the final state mesons. In Sec. 4.3 we calculate the formfactors at  $q^2 = 0$  and discuss their uncertainties. In Sec. 4.4 we present the formfactors for central input-values of the parameters and provide a simple parametrization valid in the full kinematical regime of  $q^2$ . The results for  $q^2 = 0$  are collected in Tab. 2 and Eq. (27), central results for arbitrary  $q^2$  in Tab. 3. More detailed results that allow one to determine the formfactors for arbitrary values of  $m_b$  and the Gegenbauer moments  $a_{1,2,4}$  are collected in App. A.

### 4.1 Fixing the Borel Parameter and the Continuum Threshold

We illustrate our procedure to determine  $M^2$  and  $s_0$  with the comparatively simple example of  $f_B$ , the  $B$  decay constant defined in (14). This example is actually of immediate practical use, as  $f_B$  enters our determination of the formfactors from Eq. (16). Since it is not known from experiment, its value has to be taken from theoretical calculations – which basically means either lattice determinations [19] or (local) QCD sum rules [20, 21]. To ensure consistency of our calculations, we use the values of  $f_B$  as determined from QCD sum rules to  $O(\alpha_s)$  accuracy [20]. The reason for this choice is twofold: firstly, it is

well-known that the use of  $f_B$  from sum rules reduces the dependence of the formfactors on input-parameters, in particular  $m_b$  [1]; secondly,  $O(\alpha_s^2)$  corrections to  $f_B$  turn out to be rather large [21], which was anticipated in the second reference in [20], where it was argued that these corrections are dominated by Coulombic corrections. Precisely the same corrections also enter the light-cone expansion of the correlation function  $\Pi$ , but will largely cancel in the ratio  $f_+ \sim \Pi/f_B$ . In conclusion, we expect a cancellation of both large radiative corrections and parameter dependence in the formfactors when  $f_B$  is replaced by its sum rule to  $O(\alpha_s)$  accuracy; we do not expect the resulting numerical values of  $f_B$  to be “good” predictions for that quantity.

The sum rule for  $f_B$  reads [20]<sup>5</sup>

$$f_B^2 m_B^2 e^{-\frac{m_B^2}{M^2}} = \int_{m_b^2}^{s_0} ds \rho^{\text{pert}}(s) e^{-\frac{s}{M^2}} + C_{\bar{q}q} \langle \bar{q}q \rangle + C_{\bar{q}Gq} \langle \bar{q}\sigma g Gq \rangle \equiv \int_{m_b^2}^{s_0} ds \rho^{\text{tot}}(s) e^{-\frac{s}{M^2}}. \quad (17)$$

The  $C$  are the Wilson coefficients multiplying the condensates, for which we use the following numerical values at  $\mu = 1 \text{ GeV}$ :

$$\langle \bar{q}q \rangle = -(0.24 \pm 0.01)^3 \text{ GeV}^3 \quad \text{and} \quad \langle \bar{q}\sigma g Gq \rangle = 0.8 \text{ GeV}^2 \langle \bar{q}q \rangle. \quad (18)$$

The condensates (and  $\alpha_s$ ) are actually evaluated at the scale  $M^2$ . The criteria for determining  $M^2$  and  $s_0$  are often not stated very precisely. In the present context, with many different formfactors to calculate, which entails the need for a well-defined procedure to determine the input-parameters for each of them, we decide to opt for a precisely defined method to fix the pair  $(M^2, s_0)$  and impose the following criteria on the sum rule for  $f_B$  (and, later on, the formfactors):

- the derivative of the logarithm of Eq. (17) with respect to  $1/M^2$  gives a sum rule for the  $B$  meson mass  $m_B$ :

$$m_B^2 = \int_{m_b^2}^{s_0} ds s \rho^{\text{tot}}(s) / \int_{m_b^2}^{s_0} ds \rho^{\text{tot}}(s).$$

We require this sum rule to be fulfilled to high accuracy  $\sim 0.1\%$ .

- the sum rule for  $f_B$  is required to exhibit an extremum for a given pair  $(M^2, s_0)$ .

These criteria define a set of parameters for each value of  $m_b$ , which are collected in Tab. 1, together with the resulting  $f_B$ . For all these parameter sets the continuum contribution (i.e. the integral  $\int_{s_0}^{\infty}$ ) is between 25% and 30% of the  $B$  contribution and hence well under control.

For the formfactors  $f_+^\pi$ ,  $f_0^\pi$  and  $f_T^\pi$  we follow the same procedure which results in different values of  $M^2$  and  $s_0$  for formfactors and  $f_B$ . For  $K$  and  $\eta$  we use the same values for the Borel parameter and the continuum threshold. From the explicit formulas of the tree-level sum rules for the formfactors quoted in e.g. the 3rd reference in [1], one finds that the effective Borel parameter is  $uM_{LC}^2$  rather than  $M_{LC}^2$ .<sup>6</sup> In order to keep this

<sup>5</sup>The contribution of the gluon condensate is not sizable and we therefore neglect it.

<sup>6</sup>We denote the Borel parameter of the LCSR (16) by  $M_{LC}^2$  and the Borel parameter of the SR (17) by  $M^2$ .

	$m_b$	$s_0$	$M^2$	$f_B$	$s_0^+ \approx s_0^0$	$c_c^+$	$s_0^T$	$c_c^T$
set 1	4.85	33.8	3.8	0.150	33.3	2.00	33.6	2.4
set 2	4.80	34.2	4.1	0.162	33.9	2.25	34.3	2.5
set 3	4.75	34.6	4.4	0.174	34.5	2.50	35.1	2.6
set 4	4.60	35.7	5.1	0.210	36.8	3.00	37.8	2.9

Table 1: Parameter sets for  $f_B$  and  $f(0)$ ; we use the same values of  $c_c$  and  $s_0$  for  $\pi$ ,  $K$  and  $\eta$ .  $m_b$  and  $f_B$  are given in GeV,  $s_0$  and  $M^2$  in  $\text{GeV}^2$ .

product constant, we rescale the Borel parameter by  $\langle u \rangle^{-1}$  by

$$\langle u \rangle(q^2) \equiv \int_{u_0}^{\infty} du u \phi_{\pi}(u) e^{-\frac{m_b^2 - (1-u)q^2}{uM^2}} / \int_{u_0}^{\infty} du \phi_{\pi}(u) e^{-\frac{m_b^2 - (1-u)q^2}{uM^2}}, \quad u_0 = \frac{m_b^2 - q^2}{s_0 - q^2},$$

resulting in the approximate values  $\langle u \rangle(0 \text{ GeV}^2) = 0.86$  and  $\langle u \rangle(14 \text{ GeV}^2) = 0.77$ . Parametrising the relation between the Borel parameters by

$$M_{\text{LC}}^2 \equiv c_c M^2 / \langle u \rangle, \quad (19)$$

we obtain the values and continuum thresholds given in Tab. 1.

## 4.2 Hadronic Input Parameters

The hadronic parameters needed are, for each meson, 7 parameters characterising the twist-2, 3 and 4 distribution amplitudes to NLO in the conformal expansion, cf. App. B, the decay constants of the  $\pi$ ,  $K$  and  $\eta$  and  $B$ , the factorization scale  $\mu_{\text{IR}}$ , the  $b$  quark mass  $m_b$  and the strong coupling  $\alpha_s$ . As for the latter, we fix  $\alpha_s(m_Z) = 0.118$  and use NLO evolution down to the required scale. The quark mass parameter entering our formulas is the one-loop pole mass  $m_b$  for which we use  $m_b = (4.80 \pm 0.05) \text{ GeV}$  (cf. Table 6 in the recent review [6] and references therein). We also include results for  $m_b = 4.6 \text{ GeV}$ . The infrared factorization scale separating contributions to be included in DAs and perturbatively calculable terms is chosen to be  $\mu_{\text{IR}}^2 = m_B^2 - m_b^2$ , which also sets the scale of  $\alpha_s$ ; we will discuss the residual scale-dependence of our results below. The decay constants for the  $\pi$  and  $K$  are very well known experimentally; for the  $\eta$  the situation is complicated due to  $\eta$ - $\eta'$  mixing. We use the following values:

$$f_{\pi} = 131 \text{ MeV}, \quad f_K = 160 \text{ MeV}, \quad f_{\eta} = 130 \text{ MeV}. \quad (20)$$

$f_B$  has been discussed in the previous subsection.

As for the meson DAs, we quote the preferred values for the twist-3 and 4 parameters in Tab. G; the form factors are not too sensitive to their precise values. The situation is different, however, for the Gegenbauer moments  $a_{1,2,4}(\mu)$  parametrizing the twist-2 DAs  $\phi_{\pi, K, \eta}$ , and so we shall discuss in a bit more detail what is presently known about these parameters.

Both theoretical calculations and experimental determinations focus mainly on the  $\pi$  DA (for which all odd Gegenbauer moments vanish due to G-parity; in particular

$a_1^\pi = 0$ ). The probably earliest calculation of the lowest Gegenbauer moment  $a_2$  was done by Chernyak and Zhitnitsky (CZ), yielding [22]

$$a_2^{\text{CZ}}(0.5 \text{ GeV}) = 2/3.$$

This result was obtained from local QCD sum rules, where  $a_n$  is extracted from the correlation function of the (local) interpolating field  $\bar{u}\gamma_\nu\gamma_5(\overleftrightarrow{D}\cdot x)^n d$ , where  $x$  defines the light-cone,  $x^2 = 0$ , and the usual interpolating current for the  $\pi$ ,  $\bar{u}\gamma_\mu\gamma_5 d$ . The price to pay for the expansion of an intrinsically nonlocal quantity like  $\phi_\pi$  in contributions of local operators is an increasing sensitivity to nonperturbative effects, i.e. the precise values of the condensates. As the coefficients of the condensates in the sum rule for  $a_n$  increase with powers of  $n$  and, for sufficiently large  $n$ , dominate over the perturbative contributions, it is clear that this method is inappropriate for calculating high moments, but one might expect it to be reliable at least for the lowest moment with  $n = 2$ .

The DA obtained by CZ has the remarkable feature that  $\phi_\pi(1/2, 0.5 \text{ GeV}) = 0$ , which is of course an artifact of neglecting all contributions from  $a_{n \geq 4}$ . It was subsequently shown by Braun and Filyanov (BF) [23] that both the pion-nucleon-nucleon coupling  $g_{\pi NN}$  and its mesonic equivalent  $g_{\rho\omega\pi}$ , when calculated from LCSRs, require a value of  $\phi_\pi(1/2)$  significantly different from 0 (albeit at a slightly different scale):

$$\phi_\pi(1/2, 1 \text{ GeV}) = 1.2 \pm 0.3 = \frac{3}{2} - \frac{9}{4} a_2(1 \text{ GeV}) + \frac{45}{16} a_4(1 \text{ GeV}) + \dots, \quad (21)$$

where the dots denote neglected terms in  $a_{n \geq 6}$ . The large error is due to a large sensitivity of this result to twist-4 corrections to the sum rules. BF also redetermined  $a_2$ , using the same procedure as CZ, and combining their result, which is consistent with  $a_2^{\text{CZ}}$ , with the above constraint from  $\phi_\pi(1/2)$ , they obtained

$$a_2^{\text{BF}}(1 \text{ GeV}) = 0.44, \quad a_4^{\text{BF}}(1 \text{ GeV}) = 0.25.$$

An alternative calculation aims to cure the problem of increasing condensate contributions by resumming them into nonlocal condensates [24]. The Gegenbauer moments in this approach are mostly sensitive to the ratio

$$\lambda_q^2 = \langle \bar{q}\sigma g G q \rangle / (2\langle \bar{q}q \rangle) = (0.4 \pm 0.1) \text{ GeV}^2 \quad (\mu = 1 \text{ GeV})$$

and have moderate to small values. The most recent paper on that topic, Ref. [25], quotes

$$a_2(1.16 \text{ GeV}) = 0.19, \quad a_4(1.16 \text{ GeV}) = -0.13, \quad a_{6,8,10} \sim 10^{-3}. \quad (22)$$

There are not too many lattice calculations of moments of the  $\pi$  DA. The fairly old values quoted in [26] for the 2nd moment suffer from large uncertainties. This quantity has been investigated again recently [27], but the results, obtained in quenched approximation, are still preliminary.

Alternative determinations of Gegenbauer moments rely on the analysis of experimental data, in particular the pion-photon transition formfactor  $\gamma + \gamma^* \rightarrow \pi$ , measured at CLEO and Cello, and the electromagnetic formfactor of the pion. The results of these analyses are typically either determinations of  $a_2$  (setting  $a_{n \geq 4}$  to 0) or constraints on

a linear combination of  $a_2$  and  $a_4$  (setting  $a_{n \geq 6}$  to 0).<sup>7</sup> These determinations are limited by mainly two problems: large experimental errors and the contamination by poorly known twist-4 and higher effects, which are usually estimated from QCD sum rules. As for the pion-photon transition formfactor, which has been measured by CLEO and Cello, the technique used to extract  $a_2$  and  $a_4$  has been pioneered by Khodjamirian [29], refined by Schmedding and Yakovlev [30], with subsequent further refinements by Bakulev, Mikhailov and Stefanis [31]. The upshot is that for not too small  $Q^2$  the pion-photon transition is mostly sensitive to a like-sign combination of  $a_2$  and  $a_4$ . Summarizing the analyses of this process, we conclude from Tab. I in [25] that

$$a_2(1 \text{ GeV}) + a_4(1 \text{ GeV}) = 0.1 \pm 0.1 \quad (23)$$

is a fair reflection of the current state of knowledge of  $a_{2,4}$  from that process.

As for the pion electromagnetic formfactor, the authors of Ref. [32] unfortunately only obtain a value for  $a_2$  and set  $a_4$  to zero. A very recent analysis of that formfactor, Ref. [25], concludes that calculations using the nonlocal-condensate model are in good agreement with data.

So what then do we actually know about  $a_2$  and  $a_4$ ? It seems to us that, taking everything together, and with due consideration of the respective strengths and weaknesses of different approaches, the most reliable constraints for these quantities are (21) and (23). These two constraints contain opposite-sign combinations of  $a_2$  and  $a_4$  and hence are about equally sensitive to both parameters. The resulting allowed area for  $a_2$  and  $a_4$  is shown in Fig. 2; its center is at

$$\begin{aligned} a_2(1 \text{ GeV}) &= 0.115, & a_4(1 \text{ GeV}) &= -0.015, \\ a_2(2.2 \text{ GeV}) &= 0.080, & a_4(2.2 \text{ GeV}) &= -0.0089. \end{aligned} \quad (24)$$

These are the central values we will use in our calculation of formfactors. The figure also shows that the remaining uncertainties are still considerable. Anticipating a future better determination of these parameters, from lattice or else, we will present our final results in such a way as to facilitate the inclusion of any shift in these values. Since much less is known about the Gegenbauer moments of the other pseudoscalar mesons  $K$  and  $\eta$ , we resort to SU(3) symmetry and use *the same* Gegenbauer moments.

Eq. (24) and Fig. 2 confirm the findings of previous analyses that the CZ DA is strongly disfavored; the same applies to the values obtained by BF and to the local QCD sum rule for  $a_2$ , which favors a large positive  $a_2 \sim 0.4$ . One explanation for the failure of the corresponding QCD sum rule could be that already the case  $n = 2$  may be too “nonlocal” for sum rules to work. Another one could be that the treatment of  $a_1$  and other resonances contributing to that sum rule may be insufficient. We leave a further discussion of that question to future work. The result from sum rules with nonlocal condensates [24, 25, 31], shown as black square in Fig. 2, is also outside the favored area in Fig. 2, which is mainly due to the large value of  $|a_4|$ . It would definitely be very interesting to see all these results and constraints on  $a_{2,4}$  be supplemented by lattice determinations.

---

<sup>7</sup>In principle it is possible to determine  $a_2$ ,  $a_4$  and even higher moments separately from the  $Q^2$  dependence of their respective contributions. However, such an analysis requires accurate measurements of the formfactors over a large enough range of  $Q^2$ , which are presently not available. See also Ref. [28], in particular Fig. 4.

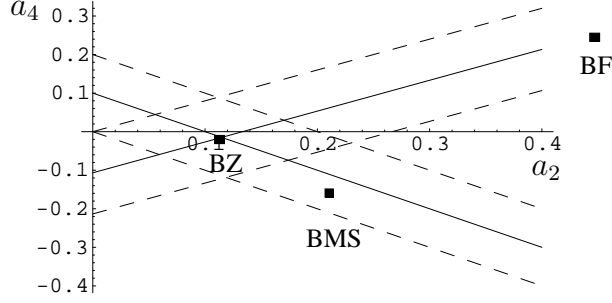


Figure 2:  $a_2(1 \text{ GeV})$  and  $a_4(1 \text{ GeV})$  as determined from the constraints (21) and (23). Solid line: central values, dashed lines: uncertainties. The black square labeled BZ denotes the central values used in this paper, Eq. (24), BMS the prediction of the nonlocal condensate model, Eq. (22), rescaled to  $\mu = 1 \text{ GeV}$ , and BF is the central value obtained in Ref. [16].

The only parameter left to discuss is  $a_1$  for the  $K$  meson (by which we understand an  $s\bar{q}$  bound state), which is a G-parity breaking parameter. Here the situation is even worse than for  $a_{2,4}$ , as neither size nor even sign of that quantity are reliably known. The facts at hand are the following: the intuitive expectation is that  $a_1$  (i.e. the moment with a weight-function proportional to  $2u - 1$ ) should be positive, as the DA is expected to be slightly tilted towards larger values of  $u$  which is the momentum fraction carried by the (heavier)  $s$  quark in the meson – the heavier the quark, the more the DA is expected to peak at large  $u$ , the extreme case being a  $b\bar{q}$  bound state whose DA should be close to  $\delta(1 - u)$ . The (tree-level) QCD sum rule calculation in [22] seemed to confirm intuition, but was challenged, when Ref. [33] found a sign-mistake in that calculation and, including two-loop radiative corrections, obtained a *negative* sign for  $a_1^K$ . For this paper, we first decided to stick to that result and use the central value  $a_1^K(1 \text{ GeV}) = -0.18$ . It turned out, however, that this value tends to produce formfactors with an unfavorable  $q^2$ -dependence.<sup>8</sup> We therefore decided to revert to the original result by CZ [22] and use

$$a_1^K(1 \text{ GeV}) = 0.17 \leftrightarrow a_1^K(2.2 \text{ GeV}) = 0.135. \quad (25)$$

The conclusion from that inconclusive situation can only be that a second opinion has to be sought, and we urge our colleagues from the lattice community to take up the challenge and provide the first-ever lattice determination of  $a_1^K$ . For the time being, we will present our results in a way that makes it possible to obtain the formfactors also for different values of  $a_1^K$ .

### 4.3 Results for $q^2 = 0$

Let us first discuss the sum rule results for  $q^2 = 0$ . They are collected in Tab. 2, for all 4 parameter sets from Tab. 1.<sup>9</sup> Including the uncertainty of  $m_b$ ,  $m_b = (4.80 \pm 0.05) \text{ GeV}$ , the final central values and uncertainties of the formfactors are given in Eq. (27).

<sup>8</sup>That is: formfactors not very compatible with the parametrization discussed in Sec. 4.4, which is based on generic analytic properties of the formfactors.

<sup>9</sup> $f_0(0)$  is not included as  $f_0(0) \equiv f_+(0)$ .

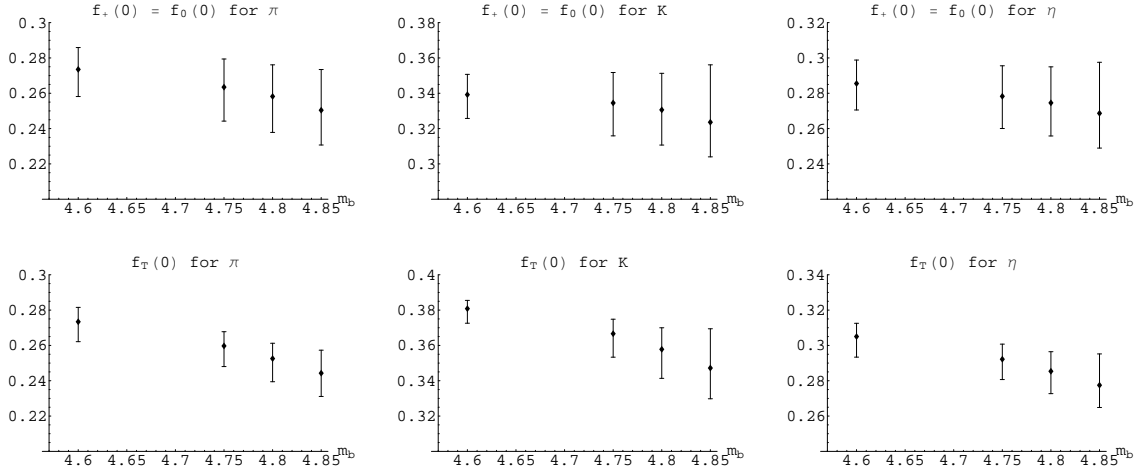


Figure 3: Central values of the formfactors  $f(0)$  and uncertainties  $\Delta$ . Numbers from Tab. 2.

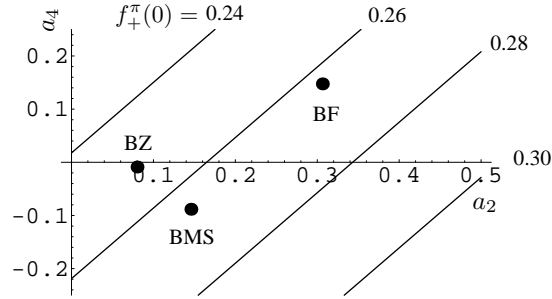


Figure 4: Dependence of  $f_+^\pi(0)$  on  $a_2(\mu_{\text{IR}})$  and  $a_4(\mu_{\text{IR}})$ , for parameter set 2. The lines are lines of constant  $f_+^\pi(0)$ . The dot labeled BZ denotes our preferred values of  $a_{2,4}$ , BMS the values from the nonlocal condensate model and BF from the sum rule calculations of Ref. [16].

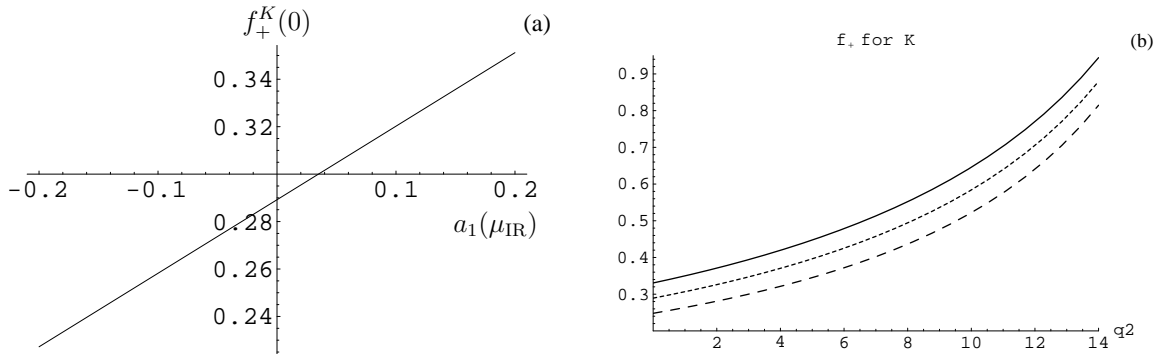


Figure 5: (a) Dependence of  $f_+^K(0)$  on the Gegenbauer moment  $a_1(\mu_{\text{IR}})$ . (b)  $f_+^K(q^2)$  as function of  $q^2$  for different values of  $a_1$ : solid line:  $a_1^K(1 \text{ GeV}) = 0.17$ , short dashes:  $a_1^K(1 \text{ GeV}) = 0$ , long dashes:  $a_1^K(1 \text{ GeV}) = -0.18$ . Input parameters: set 2.



	set 1	set 2	set 3	set 4	$\Delta_{as}$	$\Delta_{a_2,a_4}$	$\Delta$	$\Delta_{a_1}$
$f_+^\pi(0)$	0.250	0.258	0.263	0.274	0.023	0.019	0.030	—
$f_T^\pi(0)$	0.244	0.253	0.260	0.273	0.013	0.022	0.026	—
$f_+^K(0)$	0.324	0.331	0.335	0.339	0.033	0.023	0.040	$0.25\delta_{a_1}$
$f_T^K(0)$	0.347	0.358	0.367	0.381	0.022	0.027	0.035	$0.31\delta_{a_1}$
$f_+^\eta(0)$	0.269	0.275	0.278	0.286	0.029	0.019	0.035	—
$f_T^\eta(0)$	0.277	0.285	0.292	0.305	0.018	0.022	0.028	—

Table 2: Final central values of the formfactors at  $q^2 = 0$  for the parameter sets of Tab. 1.  $f_0(0) \equiv f_+(0)$ . The errors  $\Delta_{as}$ ,  $\Delta_{a_2,a_4}$  and  $\Delta_{a_1}$  are described in the text.  $\Delta$  is defined as  $\Delta = (\Delta_{as}^2 + \Delta_{a_2,a_4}^2)^{1/2}$  and  $\delta_{a_1}$  as  $\delta_{a_1} = a_1(1\text{GeV}) - 0.17$ . Note that  $\delta_{a_1}$  carries information on the sign of  $a_1$  and can become negative.

The formfactors are calculated from Eq. (16) using the parameter sets given in Tab. 1 and the hadronic input parameters given in Eqs. (24) and (25) and Tab. G. The dependence of the formfactors on  $m_b$ , i.e. the set, is shown in Fig. 3. It is evident that the residual dependence of  $f(0)$  on  $m_b$  is much smaller than the one of  $f_B$  in Tab. 2, which confirms our expectation that the calculation of  $f_B$  from a sum rule reduces the parameter dependence of the formfactors.  $f_+^\pi(0)$  depends sensitively on  $a_2$  and  $a_4$  as illustrated in Fig. 4. The formfactors show moderate SU(3) breaking between  $\pi$  and  $\eta$ , which is due to terms in the LCSRs proportional to the meson mass. For  $K$ , the situation is different, and we observe a strong enhancement of the formfactor due to the combination of two effects: the fact that  $f_K$  is larger than  $f_\pi$  and the positive contribution of the Gegenbauer moment  $a_1$  to the formfactor. As discussed in the previous subsection, the numerical value of  $a_1$ , and even its sign, is not precisely known. Fig. 5(a) illustrates the dependence of  $f_+^K(0)$  on  $a_1$ , which is quite strong. Fig. 5(b) shows the dependence of  $f_+^K(q^2)$  on  $q^2$  for different values of  $a_1$ . It is evident that  $a_1$  mainly determines the normalisation of the formfactor, but has only minor impact on its shape. The uncertainty of  $f_+^K(0)$  induced by  $a_1$  will be discussed below. The dependence of  $f_+^\pi(0)$  on the sum rule parameters  $M^2$  and  $s_0$  is illustrated in Fig. 6 and is very mild, thanks to the optimized criteria for choosing  $M^2$  and  $s_0$  outlined in Sec. 4.1. The behavior of the other formfactors is very similar. In Fig. 7 we show the variation of  $f_+^\pi(0)$  with a change of the factorization scale  $\mu_{\text{IR}}$  in the large range  $1\text{ GeV} \leq \mu_{\text{IR}} \leq m_b$ . The curve is remarkably flat which can be understood from the fact that radiative corrections cancel to a certain extent between  $\Pi_+$  and  $f_B$  and that large logarithms of type  $\ln m_b/\mu_{\text{IR}}$  occur only at subleading order in the conformal expansion of the DAs, which is numerically suppressed with respect to the leading ( $\mu_{\text{IR}}$ -independent) term, and at subleading twist, which is also suppressed.

Let us now turn to the uncertainties of the formfactors induced by a variation of the input parameters. It is convenient to split the formfactors into contributions from different Gegenbauer moments,

$$f(q^2) = f^{as}(q^2) + a_1 f^{a_1}(q^2) + \{a_2 f^{a_2}(q^2) + a_4 f^{a_4}(q^2)\}, \quad (26)$$

where  $f^{as}$  contains the contributions to the formfactors from the asymptotic DA and also

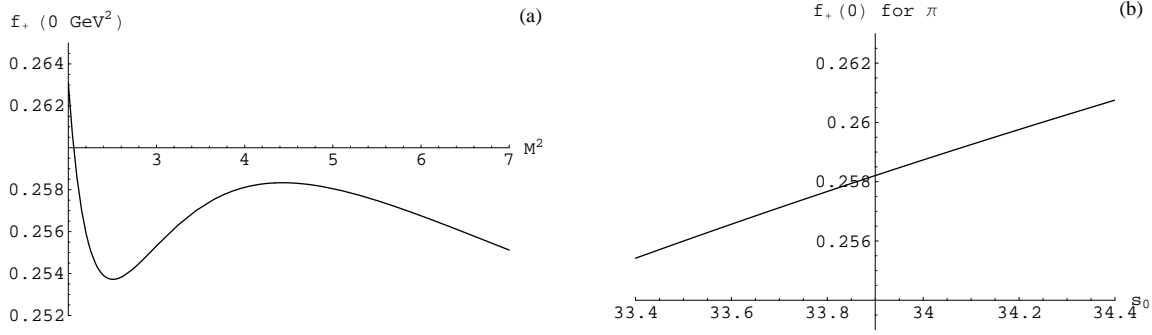


Figure 6: Dependence of  $f_+^\pi(0)$  on (a) the Borel parameter  $M^2$  and (b) the continuum threshold  $s_0$ . Input parameters: set 2 in Tab. 1.

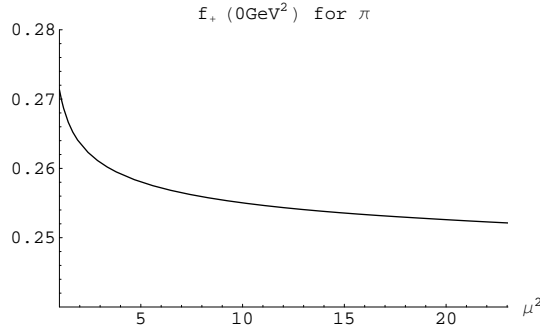


Figure 7: Dependence of  $f_+^\pi(0)$  on the factorization scale  $\mu_{\text{IR}}$ . Same input parameters as in Fig. 6.

all higher-twist effects from three-particle quark-quark-gluon matrix elements. Explicit expressions for the functions  $f^{as,a_1,a_2,a_4}$  can be obtained from Tab. C in App. A; in particular  $f^{a_i}(0)$  is just given by the parameters  $a$  in that table. We calculate separately the uncertainties  $\Delta_{as,a_1}$  of the first and second term and the combined uncertainty  $\Delta_{a_2,a_4}$  of the term in curly brackets. We start with  $\Delta_{as}$ . To estimate its value we vary the following quantities:

- the threshold  $s_0$  by  $\pm 0.5 \text{ GeV}^2$ ;
- the Borel parameter  $M^2$  in Eq. (19) by  $\pm 1.2 \text{ GeV}^2$ ;
- the infrared factorization scale  $\mu_{\text{IR}}^2 = m_B^2 - m_b^2$  by  $\pm 2 \text{ GeV}^2$ ;
- the quark condensate and the mixed condensate as indicated in Eq. (18);
- the twist-3 matrix-element  $\eta_3$  by  $\pm 50\%$ .

$m_b$  is kept fixed and we calculate the uncertainty separately for each parameter set; for a given formfactor,  $\Delta_{as}$  is then the largest uncertainty of the 4 sets. The errors are

correlated and we therefore scan the five-parameter space for the largest deviations from the central values. The resulting  $\Delta_{as}$  are given in Tab. 2.

The uncertainty of  $f^K(0)$  induced by  $a_1$  is dominated by  $a_1$  itself, so we do not attempt to determine the uncertainty of  $f^{a_1}$  arising from varying  $M^2$ ,  $s_0$  etc., but just take the maximum value of  $f^{a_1}(0) \equiv a$  from Tab. C in App. A and multiply it by  $\delta_1 = a_1(1 \text{ GeV}) - 0.17$  and the leading-order scaling factor from 1 GeV to  $\mu_{\text{IR}}$ , which gives the entry labeled  $\Delta_{a_1}$  in Tab. 2.

As the allowed input values of  $a_2$  and  $a_4$  are correlated and given by the rhomboid shown in Fig. 2, we only determine the combined uncertainty  $\Delta_{a_2, a_4}$  arising from the corresponding variation of the Gegenbauer moments, separately for each parameter set. The resulting uncertainties depend strongly on the precise values of  $M^2$  and  $s_0$ , so for a conservative estimate of the uncertainty we scan the full 7-parameter space in  $a_2$ ,  $a_4$ ,  $M^2$  etc. and quote the largest deviation from the central value as uncertainty, which yields the  $\Delta_{a_2, a_4}$  quoted in Tab. 2. Taking everything together, and including the variation of  $m_b = (4.80 \pm 0.05) \text{ GeV}$  in the error estimate, adding errors in quadrature, we find ( $\delta_{a_1}$  is defined in Tab. 2):

$f_+^\pi(0) = 0.258 \pm 0.031,$	$f_T^\pi(0) = 0.253 \pm 0.028,$	(27)
$f_+^K(0) = 0.331 \pm 0.041 + 0.25\delta_{a_1},$	$f_T^K(0) = 0.358 \pm 0.037 + 0.31\delta_{a_1},$	
$f_+^\eta(0) = 0.275 \pm 0.036,$	$f_T^\eta(0) = 0.285 \pm 0.029.$	

These are our final results for the formfactors at  $q^2 = 0$ . For  $f^{\pi, \eta}$  the total theoretical uncertainty is 10% to 13%, for  $f^K$  it is 12%, plus the uncertainty in  $a_1$ , which hopefully will be clarified through an independent calculation in the not too far future. These uncertainties include a variation of both the external input parameters and the sum rule specific parameters, but they do not include an additional “systematic” uncertainty of the sum rule method itself. To a certain extent, this intrinsic sum rule uncertainty is included by the variation of the sum rule specific parameters  $M^2$  and  $s_0$ , which sets the minimum uncertainty of the result: all external hadronic parameters fixed, this variation induces a  $\sim 7\%$  uncertainty of  $f_+^\pi(0)$  quoted in Eq. (27). Realistically, one may hope to reduce the  $\sim 12\%$  uncertainty quoted to  $\sim 10\%$  by reducing the errors on the Gegenbauer moments  $a_{2,4}$  by a factor of 2. Further improvement will then have to come from a better control over higher-twist matrix elements, dominated by the quark condensate and the quark-quark-gluon matrix element  $\eta_3$  discussed in App. B.

#### 4.4 Results for $q^2 \neq 0$ , Fits and Extrapolations

In this subsection we calculate the  $q^2$ -dependence of the formfactors for central values of the input parameters and cast them into a three-parameter parametrization that is valid for all  $q^2$ . The results are given in Tab. 3 which is to be used together with Eq. (30). The fit parameters for other sets of input parameters are given in App. A. We refrain from a complete analysis of the uncertainty of the  $q^2$ -dependence of the formfactors, but just mention that it is likely to be smaller than that at  $q^2 = 0$ , which is indicated by a decrease of the spread between the formfactors calculated from the different parameter sets in Tab. 1, cf. Fig. 9.

The validity of the LCSR approach is restricted to the kinematical regime of large meson energies,  $E_P \gg \Lambda_{\text{QCD}}$ , which via the relation

$$q^2 = m_B^2 - 2m_B E_P$$

implies a restriction to small and moderate  $q^2$ ; specifically, we evaluate the sum rules only for  $0 \leq q^2 \leq 14 \text{ GeV}^2$ . The resulting formfactors are plotted in Fig. 8, using the parameter set 2 in Tab. 1 and the hadronic input parameters given in Eqs. (24) and (25) and Tab. G. As expected from LEET [34],  $f_+$  and  $f_T$  nearly coincide. Although this agreement is expected to be best for small  $q^2$ , i.e. large energies of the light meson, it is seen to hold for all  $q^2$ . From the LCSR point of view, this agreement is due to the fact that the leading twist-2 contributions to the corresponding correlation functions coincide at tree-level. The figure also shows that the  $q^2$ -dependence of  $f_0$  is weaker than that of the other formfactors. This can be understood from the fact that, if  $f_+$  is represented as a dispersion relation over hadronic states, these states have quantum numbers  $J^P = 1^-$  and hence zero orbital angular momentum, whereas for  $f_0$  the quantum number is  $J^P = 0^+$  and thus the coupling of these states or, in the language of potential-models, their wavefunction at the origin, is suppressed as it corresponds to a state with orbital angular momentum  $L = 1$ . Fig. 8 also shows sizable SU(3) breaking for the  $K$ , but a moderate one for  $\eta$ , which is due to the same effects discussed for the formfactors at  $q^2 = 0$ . In Fig. 9 we show  $f_+^\pi(q^2)$  as function of  $q^2$ , calculated for sets 1, 3 and 4 and normalized to set 2. It is evident that the uncertainties induced by  $m_b$ , which amount to 6% at  $q^2 = 0$ , become less important for larger  $q^2$ , so that for instance the branching ratio of the semileptonic decay  $B \rightarrow \pi e \nu$  will be less dependent on the precise value of  $m_b$  than  $f_+^\pi(0)$ .

One of the main goals of this paper is to give simple expressions for the formfactors in the full physical regime  $0 \leq q^2 \leq (m_B - m_P)^2 \approx 23 \text{ GeV}^2$ . We thus have to find a parametrization that

- reproduces the data below  $14 \text{ GeV}^2$  with good accuracy;
- provides an extrapolation to  $q^2 > 14 \text{ GeV}^2$  that is consistent with the expected analytical properties of the formfactors and reproduces the lowest-lying resonance (pole) with  $J^P = 1^-$  for  $f_+$  and  $f_T$ .<sup>10</sup>

It is actually not very difficult to find good fits: the parametrization

$$f(q^2) = \frac{f(0)}{1 - a_F q^2/m_B^2 - b_F (q^2/m_B^2)^2} \quad (28)$$

advocated in previous works, e.g. [4], is one example for an excellent fit to the results of the sum rules for  $q^2 < 14 \text{ GeV}^2$ . In the present context, however, it turns out to be unsuitable as it produces, for  $f_+^\pi$ , a pole at  $q^2 \approx 23 \text{ GeV}^2$ , which is below the physical pole at  $q^2 = m_{B^*}^2 = (5.32 \text{ GeV})^2$ . In our previous paper [4] we argued that the above parametrization should be matched to a simple pole-dominance formula  $f_+ \sim 1/(m_{B^*}^2 - q^2)$  for  $q^2$  above a certain threshold  $q_0^2 \sim 15 \text{ GeV}^2$ , defined as the value of  $q^2$  that would allow a

---

<sup>10</sup>For  $f_0$ , the lowest pole with quantum numbers  $0^+$  lies above the two-particle threshold starting at  $(m_B + m_P)^2$  and hence is not expected to feature prominently.

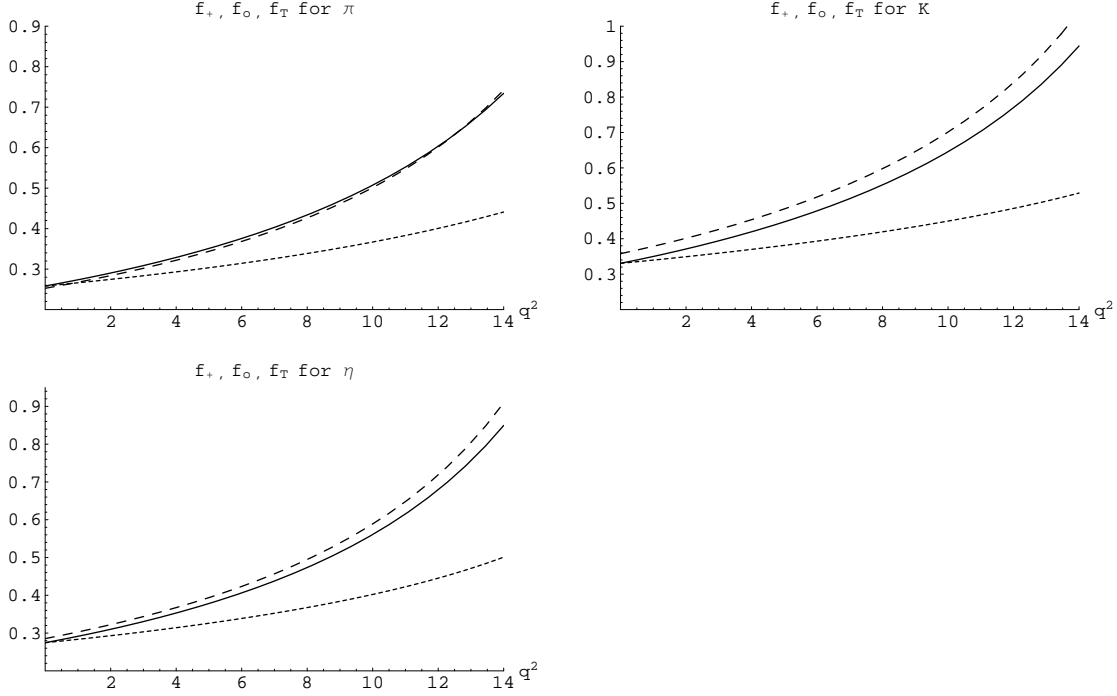


Figure 8:  $f_+$  (solid lines),  $f_0$  (short dashes) and  $f_T$  (long dashes) as functions of  $q^2$  for  $\pi$ ,  $K$  and  $\eta$ . The renormalisation scale of  $f_T$  is chosen to be  $m_b$ . Input parameters: set 2 in Tab. 1.

smooth transition<sup>11</sup> from one parametrization to the other. This procedure unfortunately does not work for our new formfactors, as the optimum  $q_0^2$  turns out to be far outside the physical regime. We therefore decide to follow, as far as possible, the procedure advocated by Becirevic and Kaidalov [35], who suggested to write the formfactor  $f_+$  as dispersion relation in  $q^2$  with a lowest-lying pole plus a contribution from multiparticle states, which in turn is to be replaced by an effective pole at higher mass:

$$f_+(q^2) = \frac{r_1}{1 - q^2/m_1^2} + \int_{(m_B+m_P)^2}^{\infty} ds \frac{\rho(s)}{s - q^2} \quad (29)$$

$$\rightarrow \frac{r_1}{1 - q^2/m_1^2} + \frac{r_2}{1 - q^2/m_{\text{fit}}^2}. \quad (30)$$

The lowest-lying resonance in the  $b\bar{u}$  channel is well known experimentally: it the  $B^*(1^-)$  vector meson with mass 5.32 GeV; this is also the mass to be used for the  $\eta$ , as the  $B \rightarrow \eta$  formfactors calculated in this paper refer to a  $b \rightarrow u$  transition. For the  $K$  we have calculated the mass of the  $B_s^*$  resonance in the heavy-quark limit and find

$$m_{B_s^*}^2 - m_{B_s}^2 = m_{B^*}^2 - m_B^2 \quad \rightarrow \quad m_1^K = m_{B_s^*} = 5.41 \text{ GeV}.$$

For Eq. (30) to describe all  $f_+$  and also  $f_T$ , which feature the same  $1^-$  resonance, in terms of three fit parameters,  $r_1$ ,  $r_2$  and  $m_{\text{fit}}$ , it is crucial that the position of the

<sup>11</sup>That is equality of both the parametrization formulas and their first derivatives in  $q_0^2$ .

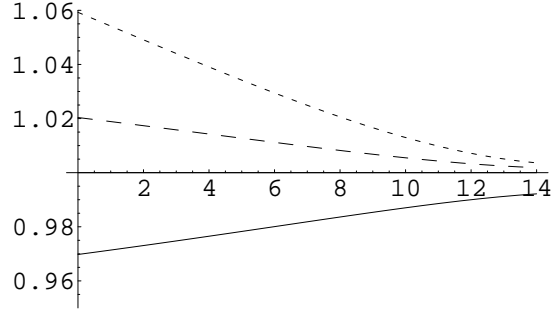


Figure 9: Ratio of  $f_+^{\pi(\text{set } i)}(q^2)/f_+^{\pi(\text{set } 2)}(q^2)$  as function of  $q^2$ . Solid line: set 1; long dashes: set 3; short dashes: set 4.

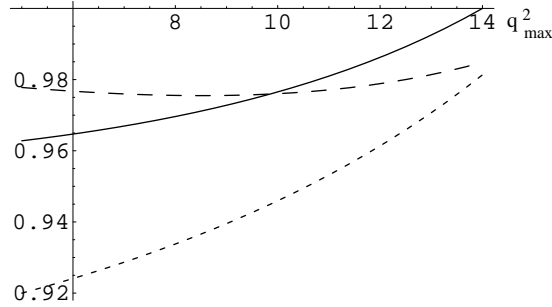


Figure 10: Variation of the total semileptonic rate  $\Gamma(B \rightarrow \pi e \nu)$  as function of  $q_{\text{max}}^2$ , the maximum  $q^2$  for which LCSR results are included in the fits. The rate is normalized to 1 for  $q_{\text{max}}^2 = 14 \text{ GeV}^2$  and fit 1. Solid line: fit 1, long dashes: fit 2, short dashes: fit 3. Input parameters: set 2.

lowest pole is sufficiently below the two-particle cut starting at  $(m_B + m_P)^2$ . We find that indeed most  $f_{+,T}^{\pi}$  formfactors, with the exception of  $f_T^{\pi(\text{set } 4)}$ , are described very well by (30). For  $f_T^{\pi(\text{set } 4)}$ , however, and all  $f_{+,T}^{K,\eta}$ ,  $m_{\text{fit}}$  gets too close to  $m_1$ , so that the fit becomes numerically unstable. In this case, it is appropriate to expand (30) to first order in  $m_{\text{fit}} - m_1$ , which yields

$$f_{+,T}^{K,\eta}(q^2) = \frac{r_1}{1 - q^2/m_1^2} + \frac{r_2}{(1 - q^2/m_1^2)^2} \quad (31)$$

with fit parameters  $r_1$  and  $r_2$ , and  $m_1 = m_{B^*,B_s^*}$  fixed.

For  $f_0$ , one can write a decomposition similar to (29), but here the lowest-lying pole with quantum numbers  $0^+$  lies either above the two-particle threshold (for  $\pi$  and  $\eta$ ) or is very close to it (for  $K$ , cf. Tab. D), so that the pole is effectively hidden under the cut and only the dispersive term survives in (29). We again follow the suggestion of Becirevic and Kaidalov and replace this term by an effective pole, i.e. we set

$$f_0(q^2) = \frac{r_2}{1 - q^2/m_{\text{fit}}^2}. \quad (32)$$

The accuracy of the fits of the LCSR results to the above parametrizations is generally very high and best for sets 1 to 3 of Tab. 1 with  $m_b = (4.80 \pm 0.05) \text{ GeV}$ , with a maximum

	$r_1$	$r_2$	$(m_1)^2$	$m_{\text{fit}}^2$
$f_+^\pi$	0.744	-0.486	$(m_1^\pi)^2$	40.73
$f_0^\pi$	0	0.258	—	33.81
$f_T^\pi$	1.387	-1.134	$(m_1^\pi)^2$	32.22
$f_+^K$	0.162	0.173	$(m_1^K)^2$	—
$f_0^K$	0	0.330	—	37.46
$f_T^K$	0.161	0.198	$(m_1^K)^2$	—
$f_+^\eta$	0.122	0.155	$(m_1^\eta)^2$	—
$f_0^\eta$	0	0.273	—	31.03
$f_T^\eta$	0.111	0.175	$(m_1^\eta)^2$	—

Table 3: Fit parameters for Eq. (30) for set 2 in Tab. 1 and central values of the input parameters of the DAs, Eqs. (24), (25) and Tab. G.  $m_1$  is the vector meson mass in the corresponding channel:  $m_1^{\pi,\eta} = m_{B^*} = 5.32 \text{ GeV}$  and  $m_1^K = m_{B_s^*} = 5.41 \text{ GeV}$ . The scale of  $f_T$  is  $\mu = 4.8 \text{ GeV}$ .

	set 1	set 2	set 3	set 4
fit 1	0.97	1	1.01	1.05
fit 2	0.97	0.98	0.99	1.00
fit 3	0.95	0.98	1.00	1.04

Table 4: Total semileptonic decay rates  $\Gamma(B \rightarrow \pi e \nu)$  normalised to 1 for set 2, fit 1, for different formfactor parametrizations and input parameter sets.

1.2% deviation; set 4 fares slightly worse with an accuracy of 2% or better. The quality of the fits is discussed in more detail in App. A. The uncertainty introduced by fitting is much smaller than the actual uncertainty of the sum rule calculation, which we have found to be around 10% at  $q^2 = 0$ , and also much smaller than the intrinsic and irreducible sum rule uncertainty, which we have estimated to be  $\sim 7\%$ . Nevertheless it is legitimate to ask whether the extrapolation of the fits to  $q^2 > 14 \text{ GeV}^2$ , or the variation of the “cutoff”  $q_{\text{max}}^2 = 14 \text{ GeV}^2$ , introduce an additional uncertainty. In answering this question, we first would like to recall that for most applications it is actually sufficient to know the formfactors for  $q^2 < 14 \text{ GeV}^2$  only — these include in particular nonleptonic  $B$  decays treated in QCD factorization, and also the rare decays  $B \rightarrow (\pi, K, \eta) \ell^+ \ell^-$ , as the spectrum for invariant lepton masses above the  $c\bar{c}$  threshold, i.e.  $q^2 \geq m_{J/\psi}^2 \approx 10 \text{ GeV}^2$ , is dominated by long-distance processes unrelated to  $B \rightarrow (\pi, K, \eta)$  formfactors. The only, but very important case where the formfactor is needed over the full range of  $q^2$  is the semileptonic decay  $B \rightarrow \pi \ell \nu$ , which depends on  $f_+^\pi$  and (for decays into  $\tau$ ) on  $f_0^\pi$ . We discuss the effect of the extrapolation on this decay by studying three different parametrizations of  $f_+^\pi$ :

fit 1: Eq. (30), our standard parametrization;



fit 2: a modified version of (28), with one zero of the denominator fixed at  $m_1^2 = m_{B^*}^2$ :

$$f_+^\pi(q^2) = \frac{f_+^\pi(0)}{(1 - q^2/m_1^2)(1 - q^2/m_{\text{fit}}^2)};$$

fit 3: a parametrization similar to (31), but with the pole mass as fit parameter:

$$f_+^\pi(q^2) = \frac{r_1}{1 - q^2/m_{\text{fit}}^2} + \frac{r_2}{(1 - q^2/m_{\text{fit}}^2)^2}.$$

We quantify the difference between these parametrizations by calculating the semileptonic decay rate, the integral of Eq. (4) over  $q^2$  from 0 to  $(m_B - m_\pi)^2$ , normalizing to our central values, set 2 and fit 1. The results are collected in Tab. 4. It is evident that the dependence of the rate on the fit is rather mild, despite the double-pole of fit 3, which is however sufficiently far away from the endpoint of the spectrum,  $m_{\text{fit}} = (5.6 \pm 0.1)$  GeV, and hence has only moderate impact on the rate. We conclude that the extrapolation of  $f_+^\pi$  causes an uncertainty in the total semileptonic decay rate  $\Gamma(B \rightarrow \pi e \nu)$  which is considerably less than the expected intrinsic sum rule uncertainty of  $\sim 14\%$ .

We conclude the discussion of the uncertainty of the extrapolations by studying the effect of changing the maximum value of  $q^2$  for which the sum rules results are included in the fits. Our default value  $q_{\text{max}}^2$  is  $14 \text{ GeV}^2$ ; lowering  $q_{\text{max}}^2$  changes the fit parameters of all three parametrizations and hence the predictions for the total semileptonic decay rate. Fig. 10 shows the corresponding change in the rate, normalised to our central values fit 1 and  $q_{\text{max}}^2 = 14 \text{ GeV}^2$ . Again the dependence of the rate on  $q_{\text{max}}^2$  is mild, which corroborates our conclusion that the precise shape of the formfactor is not that relevant, as long as it does not exhibit too strong a singularity at  $q^2 = (5.32 \text{ GeV})^2$ .

There are also other tests and checks for the validity of the extrapolation of (30) to the full physical regime  $q^2 < (m_B - m_P)^2$ : firstly, the coefficient  $r_1$  for  $f_+^\pi$  is related to the coupling  $g_{BB^*\pi}$  as

$$r_1 = \frac{f_{B^*} g_{BB^*\pi}}{2m_{B^*}}. \quad (33)$$

At the upper end of the physical range in  $q^2$  we can expect vector-meson dominance to be effective and therefore the fit-parameter should be close to the above value. In fact lattice [36] and meson-loop calculations (cf. the first reference in [6]) yield  $r_1 \approx 0.8$ , but are at variance with a determination of  $g_{BB^*\pi}$  from LCSRs which yields  $r_1 \approx 0.44$  [5]. The lattice and meson-loop calculations are further supported by the agreement of their predictions for  $g_{DD^*\pi}$  with experimental measurements, whereas LCSRs again give a value that is too low by almost a factor of two. The author of [37] speculates that this discrepancy may be explained by a violation of quark-hadron duality in the LCSRs used for the determination of  $g_{DD^*\pi}$  and  $g_{BB^*\pi}$ , which would preclude a clean determination of these couplings from LCSRs. Another possible solution of the problem was suggested in Ref. [38], where it was shown that the value of  $r_1$  from LCSRs increases once a radial excitation with negative residue is included in the hadronic parametrization of the correlation function.<sup>12</sup> If we interpret our fit results as determinations of  $g_{BB^*\pi}$ , we get the following values of  $r_1$  for

---

<sup>12</sup>Note that the corresponding spectral function is not positive definite.

the sets 1 to 4: (0.73,0.74,0.77,0.94) (cf. Tab. A), which is in reasonable agreement with lattice and meson-loop calculations.

Secondly, there is one further constraint on the formfactor  $f_0$ . As first pointed out in Ref. [39], in the soft-pion limit  $p \rightarrow 0$  and  $m_\pi^2 \rightarrow 0$  (i.e.  $q^2 = m_B^2$ )  $f_0^\pi(m_B^2)$  is related to the decay constants of the  $B$  and  $\pi$  as

$$f_0^\pi(m_B^2) = \frac{f_B}{f_\pi}. \quad (34)$$

We can compare this relation with our parametrization by solving it for  $f_B$ . For the four parameter sets of Tab. 1, we get from Eq. (34)  $f_B^{\text{set1}} = 201 \text{ MeV}$ ,  $f_B^{\text{set2}} = 193 \text{ MeV}$ ,  $f_B^{\text{set3}} = 190 \text{ MeV}$  and  $f_B^{\text{set4}} = 207 \text{ MeV}$ , which is in good agreement with lattice and sum rule calculations.

Let us conclude with one more remark. In LEET,  $f_+$  and  $f_0$  are related as [34]:

$$f_0 = \frac{2E}{m_B} f_+, \quad (35)$$

which is valid in the combined limits  $m_B \rightarrow \infty$  and  $E \rightarrow \infty$ . This constraint was used in Ref. [35] to reduce the number of fit parameters to two as necessitated by the limited accuracy of the lattice formfactors. We do not impose this constraint explicitly, but find that it is valid to 4% accuracy for our formfactors, for not too large  $q^2$ .

Summarizing, we conclude that, for all formfactors, the three-parameter formula (30) provides both an excellent fit to the LCSR results for  $q^2 < 14 \text{ GeV}^2$  and a smooth extrapolation to  $14 \text{ GeV}^2 < q^2 < (m_B - m_P)^2$ , and is consistent with all known constraints.

## 5 Summary & Conclusions

In this paper we have given a thorough and careful examination of the predictions of QCD sum rules on the light-cone for the formfactors  $f_+$ ,  $f_0$  and  $f_T$  for the decays  $B \rightarrow \pi, K, \eta$ . We have not discussed  $B \rightarrow \eta'$ , which is not accessible within the method due to its large mass.

The main improvements of our results with respect to our previous publications [3, 4] are:

- predictions for all formfactors of  $B \rightarrow \pi, K, \eta$  transitions to  $O(\alpha_s)$  accuracy for twist-2 and 3 two-particle contributions;
- a well-defined and precise method for fixing sum rule specific parameters (cf. Sec. 4.1);
- a careful assessment of uncertainties at zero momentum transfer (cf. Sec. 4.2 and 4.3);
- a detailed breakdown of the contributions of different Gegenbauer moments  $a_i$  to the formfactors (cf. App. A), which
  - renders straightforward the implementation of future updates of these parameters;

- allows the assessment of the impact of nonasymptotic twist-2 distribution amplitudes on QCD factorised nonleptonic B decays in a coherent way, to 4th order in the conformal expansion;
- a parametrization of the  $q^2$ -dependence of formfactors valid in the full physical regime of momentum transfer that reproduces all relevant analytical properties of the formfactors (cf. Sec. 4.4).

Our main results for  $q^2 = 0$  are collected in Tab. 2 and Eq. (27). They depend crucially on the values of the Gegenbauer moments describing the twist-2 distribution amplitudes of  $\pi$ ,  $K$  and  $\eta$ , cf. App. B. We have determined these parameters as discussed in Sec. 4.2, but a better determination from an independent source, e.g. lattice calculations, would be extremely useful. This applies in particular to the SU(3) breaking parameter  $a_1^K$ , whose size and even sign is under discussion (cf. Ref. [33]). Once more precise values for these parameters will be available, it is straightforward to obtain the corresponding formfactors from the data collected in App. A. Setting aside  $a_1$ , the total theoretical uncertainty of the formfactors at  $q^2 = 0$  is 10% to 13%, which includes a variation of all input parameters. It can be further improved by reducing the uncertainties of, in particular,  $a_2$ ,  $a_4$ , the quark condensate and  $\eta_3$ , the dominant quark-quark-gluon matrix element. A reduction of the uncertainty of  $a_{2,4}$  by a factor of two will give a  $\sim 2\%$  gain in accuracy, reducing the uncertainty of the quark condensate and  $\eta_3$  by the same factor will give another 2%. The uncertainty due to the variation of only the sum rule specific parameters is 7%, which cannot be reduced any further and hence sets the minimum theoretical uncertainty that can be achieved within this method. Comparing with the uncertainties quoted in our previous publications, we have achieved a reduction of the global estimate  $\sim 15\%$  quoted in [3] and also of the 20% uncertainty for  $f_+^\pi(0)$  quoted in [4]. This is partially due to a reduction of the uncertainties of the hadronic input parameters, in particular  $m_b$ , and partially due to a refinement of the assessment of sum rule specific uncertainties as discussed in Sec. 4.1.

We have also calculated all formfactors for  $0 \leq q^2 \leq 14 \text{ GeV}^2$ ; the upper bound on  $q^2$  is due to the limitations of the light-cone expansion which requires the final-state meson to have energies  $E \gg \Lambda_{\text{QCD}}$ : for  $q_{\text{max}}^2 = 14 \text{ GeV}^2$  the meson energy is  $E = 1.3 \text{ GeV}$ . In order to allow a simple implementation of our results, we have given a parametrisation that includes the main features of the analytical properties of the formfactors and is valid in the full physical regime  $0 \leq q^2 \leq (m_B - m_P)^2$ . The corresponding results for our preferred set of input parameters are given in Tab. 3; a detailed breakdown of the contributions of different parameters to the full formfactors is given in App. A. The main features of the results are that the formfactors  $f_+$  and  $f_T$  are nearly equal as predicted by LEET and that  $f_0$  is very well described by a single-pole formula. The uncertainty induced by the extrapolation of the parametrization to larger momentum transfers is an issue only for the semileptonic decay  $B \rightarrow \pi e \nu$ ; we have checked that the change of the total rate is at most 5% for three different extrapolations of the light-cone sum rule results.

Our approach is complementary to standard lattice calculations, in the sense that it works best for large energies of the final state meson (i.e. small  $q^2$ ), whereas lattice calculations work best for small energies – a situation that may change in the future with the implementation of moving NRQCD [10]. Previously, the LCSR results for  $f_{+,0}^\pi$  at

	set 2, $m_b = 4.8 \text{ GeV}$					set 4, $m_b = 4.6 \text{ GeV}$				
	$r_1$	$m_1^2$	$r_2$	$m_{\text{fit}}^2$	$\Delta$	$r_1$	$m_1$	$r_2$	$m_{\text{fit}}^2$	$\Delta$
$f_+^\pi$	0.744	$(m_1^\pi)^2$	-0.486	40.73	0.3	0.944	$(m_1^\pi)^2$	-0.669	34.27	0.3
$f_0^\pi$	0	—	0.258	33.81	0.1	0	—	0.270	33.63	1.2
$f_T^\pi$	1.387	$(m_1^\pi)^2$	-1.134	32.22	0.5	use (A.2) with $r_1 = 0.152$ , $r_2 = 0.122, m_1 = m_1^\pi, \Delta = 0.4$				
$f_+^{\pi,as}$	0.918	$(m_1^\pi)^2$	-0.675	38.20	0.1	0.711	$(m_1^\pi)^2$	-0.441	44.31	0.1
$f_0^{\pi,as}$	0	—	0.244	30.46	0.8	0	—	0.270	31.93	0.1
$f_T^{\pi,as}$	1.556	$(m_1^\pi)^2$	-1.321	32.56	0.2	1.331	$(m_1^\pi)^2$	-1.061	33.43	0.4

Table A: Fit parameters for the  $\pi$  Eq. (A.1) for both the full formfactors and the asymptotic ones,  $f^{as}$ , Eq. (A.5), using the sets 2 and 4 in Tab. 1. The formfactor  $f_0$  is fitted to the parametrization (A.3). The mass parameters  $m_1^x$  are given in Tab. D.  $\Delta$  is a measure of the quality of the fit and is defined in (A.4).

small and moderate  $q^2$  were found to nicely match the lattice results obtained for large  $q^2$  [42]. The situation will have to be reassessed in view of our new results and it will be very interesting to see if and how it will develop with further progress in both lattice and LCSR calculations.

## Acknowledgements

R.Z. is grateful to M.B. Voloshin for clarifications; he is supported by the Swiss National Science Foundation. P.B. would like to thank the W.I. Fine Theoretical Physics Institute at the University of Minnesota in Minneapolis for hospitality while this paper was semi-finalised.

## Appendix

### A Fit Parameters and Comments

This appendix extends the discussion of Sec. 4.4.

**Full formfactors.** As discussed in Sec. 4.4, we fit the LCSR results to the following parametrizations:

- for  $f_{+,T}^\pi$ :<sup>13</sup>

$$f(q^2) = \frac{r_1}{1 - q^2/m_1^2} + \frac{r_2}{1 - q^2/m_{\text{fit}}^2} \quad , \quad (\text{A.1})$$

---

<sup>13</sup>Apart from  $f_T^\pi$  for set 4, which shows the same behavior as  $f_{+,T}^{K,\eta}$  and hence is parametrised the same way, i.e. according to (A.2).

	set 2, $m_b = 4.8 \text{ GeV}$				set 4, $m_b = 4.6 \text{ GeV}$			
	$r_1$	$r_2$	$m_{\text{fit}}(m_1)$	$\Delta$	$r_1$	$r_2$	$m_{\text{fit}}(m_1)$	$\Delta$
$f_+^K$	0.1616	0.1730	$(m_1^K)^2$	1.2	0.1903	0.1478	$(m_1^K)^2$	1.0
$f_0^K$	0	0.3302	37.46	1.0	0	0.3338	38.98	1.9
$f_T^K$	0.1614	0.1981	$(m_1^K)^2$	0.5	0.1851	0.1905	$(m_1^K)^2$	1.7
$f_+^\eta$	0.1220	0.1553	$(m_1^\eta)^2$	1.0	0.1380	0.1462	$(m_1^\eta)^2$	0.9
$f_0^\eta$	0	0.2734	31.03	0.5	0	0.2799	30.46	2.0
$f_T^\eta$	0.1108	0.1752	$(m_1^\eta)^2$	0.5	0.1160	0.1841	$(m_1^\eta)^2$	1.6
$f_+^{K,as}$	0.0541	0.2166	$(m_1^K)^2$	0.2	0.0991	0.2002	$(m_1^K)^2$	0.6
$f_0^{K,as}$	0	0.2719	30.33	0.7	0	0.2984	31.99	0.5
$f_T^{K,as}$	0.0244	0.2590	$(m_1^K)^2$	0.8	0.0660	0.2621	$(m_1^K)^2$	1.3
$f_+^{\eta,as}$	0.0802	0.1814	$(m_1^\eta)^2$	1.0	0.1201	0.1636	$(m_1^\eta)^2$	0.6
$f_0^{\eta,as}$	0	0.2604	28.80	0.5	0	0.2803	29.59	0.8
$f_T^{\eta,as}$	0.0570	0.2115	$(m_1^\eta)^2$	0.3	0.0914	0.2096	$(m_1^\eta)^2$	1.0

Table B: Fit parameters for  $K$  and  $\eta$  for Eq. (A.2), for both the full formfactors and the asymptotic ones,  $f^{as}$ , Eq. (A.5), using the sets 2 and 4 in Tab. 1. The formfactor  $f_0$  is fitted to the parametrisation A.3. The mass parameters  $m_1$  are given in Tab. D.  $\Delta$  is a measure of the quality of the fit and is defined in (A.4).

where  $m_1^\pi$  is the mass of  $B^*(1^-)$ ,  $m_1^\pi = 5.32 \text{ GeV}$ ; the fit parameters are  $r_1$ ,  $r_2$  and  $m_{\text{fit}}$ ;

- for  $f_{+,T}^{K,\eta}$  and  $f_T^\pi$  (set 4):

$$f(q^2) = \frac{r_1}{1 - q^2/m_1^2} + \frac{r_2}{(1 - q^2/m_1^2)^2}, \quad (\text{A.2})$$

where  $m_1$  is the mass of the  $1^-$  meson in the corresponding channel, cf. Tab. D; the fit parameters are  $r_1$  and  $r_2$ ;

- for  $f_0$ :

$$f_0(q^2) = \frac{r_2}{1 - q^2/m_{\text{fit}}^2}, \quad (\text{A.3})$$

the fit parameters are  $r_2$  and  $m_{\text{fit}}$ .

The fit parameters are collected in the upper halves of Tabs. A and B.  $\Delta$  is a measure of the quality of the fit and defined as

$$\Delta = 100 \max_t \left| \frac{f(t) - f^{\text{fit}}(t)}{f(t)} \right|, \quad t \in \{0, \frac{1}{2}, \dots, \frac{27}{2}, 14\} \text{ GeV}^2, \quad (\text{A.4})$$

i.e. it gives, in per cent, the maximum deviation of the fitted formfactors from the original LCSR result for  $q^2 < 14 \text{ GeV}^2$ . From the  $\Delta$  given in the table we conclude that the overall quality of the fits is very good and best for the pion and also that they work better for our preferred set 2 than for set 4.

	set 2, $m_b=4.8$ GeV					set 4, $m_b=4.6$ GeV				
	$a$	$b \times 10^2$	$c \times 10^2$	$d \times 10^3$	$\delta$	$a$	$b \times 10^2$	$c \times 10^2$	$d \times 10^3$	$\delta$
$f_+^K(a_1)$	0.310	0.930	0.139	-0.083	0.3	0.276	0.060	0.151	-0.157	0.7
$f_0^K(a_1)$	0.308	0.106	0.026	-0.048	0.2	0.273	-0.433	0.0001	-0.051	0.2
$f_T^K(a_1)$	0.381	1.056	0.167	-0.108	0.3	0.354	0.027	0.178	-0.194	0.7
$f_+^\pi(a_2)$	0.187	-0.517	0.014	-0.117	0.5	0.040	-0.762	-0.201	0.050	1.5
$f_0^\pi(a_2)$	0.185	-0.841	-0.075	-0.005	0.4	0.041	-1.078	-0.123	0.068	1.2
$f_T^\pi(a_2)$	0.203	-0.659	-0.008	-0.118	0.3	0.038	-0.944	-0.244	0.073	1.5
$f_+^K(a_2)$	0.228	-0.632	0.017	-0.143	0.5	0.049	-0.931	-0.245	0.061	1.5
$f_0^K(a_2)$	0.226	-1.031	-0.092	-0.005	0.4	0.050	-1.32	-0.150	0.083	1.2
$f_T^K(a_2)$	0.264	-0.858	-0.011	-0.153	0.3	0.049	-1.228	-0.318	0.095	1.5
$f_+^\eta(a_2)$	0.185	-0.514	0.014	-0.116	0.5	0.039	-0.757	-0.199	0.049	1.5
$f_0^\eta(a_2)$	0.183	-0.829	-0.076	-0.002	0.4	0.041	-1.068	-0.122	0.069	1.2
$f_T^\eta(a_2)$	0.216	-0.722	-0.007	-0.128	0.3	0.040	-1.019	-0.259	0.076	1.4
$f_+^\pi(a_4)$	-0.141	-0.775	0.004	0.161	0.7	-0.054	-0.506	0.621	-0.326	5.2
$f_0^\pi(a_4)$	-0.139	-0.687	0.170	0.002	1.5	-0.061	0.703	0.323	-0.209	2.9
$f_T^\pi(a_4)$	-0.167	-0.895	0.077	0.143	1.1	-0.047	-0.327	0.698	-0.394	4.9
$f_+^K(a_4)$	-0.173	-0.947	0.005	0.196	0.7	-0.067	-0.618	0.759	-0.398	5.2
$f_0^K(a_4)$	-0.170	-0.838	0.209	0.001	1.5	-0.075	0.871	0.392	-0.254	2.9
$f_T^K(a_4)$	-0.217	-1.165	0.101	0.187	1.1	-0.061	-0.426	0.909	-0.513	4.9
$f_+^\eta(a_4)$	-0.140	-0.770	0.004	0.159	0.7	-0.054	-0.502	0.616	-0.323	5.2
$f_0^\eta(a_4)$	-0.138	-0.681	0.170	0.0005	1.5	-0.061	0.710	0.318	-0.206	2.9
$f_T^\eta(a_4)$	-0.178	-0.955	0.083	0.153	1.1	-0.050	-0.349	0.745	-0.421	4.9

Table C: Fit parameters for Eq. (A.6) for the functions  $f^{a_i}$  defined in (A.5).  $\delta$  is a measure of the quality of the fit and defined in (A.7).

**Split formfactors.** As discussed in Sec. 4.2, the values of the Gegenbauer moments  $a_{1,2,4}$  are not very well known. In Sec. 4.4 and Tabs. A, B we have presented results only for our preferred choice of these parameters, i.e.

$$\begin{aligned}
a_1^K(1 \text{ GeV}) &= 0.17, & a_2^{\pi,K,\eta}(1 \text{ GeV}) &= 0.115, & a_4^{\pi,K,\eta}(1 \text{ GeV}) &= -0.015, \\
a_1^K(2.2 \text{ GeV}) &= 0.135, & a_2^{\pi,K,\eta}(2.2 \text{ GeV}) &= 0.080, & a_4^{\pi,K,\eta}(2.2 \text{ GeV}) &= -0.0089;
\end{aligned}$$

for set 4, the  $a_i$  are scaled up to  $\mu_{\text{IR}} = 2.6 \text{ GeV}$ . In order to allow the inclusion of future updates of these values, we split the formfactors into contributions from different Gegenbauer moments. We define<sup>14</sup>

$$f(q^2) = f^{as}(q^2) + a_1(\mu_{\text{IR}})f^{a_1}(q^2) + a_2(\mu_{\text{IR}})f^{a_2}(q^2) + a_4(\mu_{\text{IR}})f^{a_4}(q^2), \quad (\text{A.5})$$

<sup>14</sup>Note that this splitting is exact and valid for arbitrarily large  $a_i$  — there are no nonlinear terms in  $a_i$ .

	$m_1^2 \quad (1^-)$	$m_{1*}^2 \quad (0^+)$	$q_{\max}^2$
$\pi (\eta)$	$5.32^2 = 28.4$	$5.63^2 = 31.7$	26.4 (22.8)
$K$	$5.41^2 = 29.3$	$5.72^2 = 32.7$	23.8

Table D: Masses of  $1^-$  and  $0^+$  resonances in the  $b\bar{u}$  and  $b\bar{s}$  channels. The  $1^-$  masses are obtained from experiment and heavy-quark relations, the  $0^+$  masses from a potential model [40]. All numbers in units  $\text{GeV}^2$ .

where  $f^{as}$  contains twist-2 contributions from the asymptotic DA and also all higher-twist contributions not proportional to  $a_{1,2,4}$ . The task is now to fit all functions  $f^{as, a_1, a_2, a_4}$ , in the interval  $0 < q^2 < 14\text{GeV}^2$ , to appropriate parametrizations.

For  $f^{as}$ , which gives the dominant contribution to all formfactors, we use the same parametrisation as for the full formfactors. The results are collected in the lower halves of Tabs. A and B. Again, the fits are very good and best for the pion and set 2.

The  $f^{a_i}$  turn out to be slowly varying functions of  $q^2$ , which can be fitted by a polynomial of 3rd degree:

$$f^{a_i}(q^2) = a + b(q^2) + c(q^2)^2 + d(q^2)^3 \quad . \quad (\text{A.6})$$

The measure of the quality of the fit has now to be defined in a slightly different way, as the  $f^{a_i}$  have zeros in the fit interval. We define the fit-quality  $\delta$  as

$$\delta = 100 \frac{\sum_t |f(t) - f^{\text{fit}}(t)|}{\sum_t |f(t)|}, \quad t \in \{0, \frac{1}{2}, \dots, \frac{27}{2}, 14\} \text{ GeV}^2, \quad (\text{A.7})$$

i.e. as the average deviation of the fit from the true value, in per cent. The fit parameters are given in Tab. C. As one can read off from the  $\delta$ 's, the fits are best for  $f^{a_1}$ , still good for  $f^{a_2}$  and worst for  $f^{a_4}$ . The limited quality of the fits for  $f^{a_4}$  is due to a change of sign of its derivative at the upper end of the fit interval, which cannot be reliably reproduced by a polynomial of 3rd degree.

We would like to stress that none of the split-formfactor parametrizations must be used for  $q^2$  larger than  $14\text{GeV}^2$ . For calculating the full formfactors for arbitrary  $a_{1,2,4}$ , the following procedure should be followed:

- determine  $a_{1,2,4}$  at the scale  $\mu_{\text{IR}}^2 = m_B^2 - m_b^2$ ; the scaling factors from  $\mu = 1\text{ GeV}$  up to  $2.2\text{ GeV}$  (i.e.  $m_b = 4.8\text{ GeV}$ ) are (0.793, 0.696, 0.590) for  $(a_1, a_2, a_4)$ ;
- choose set 2 (preferred) or set 4;
- calculate  $f^{as}$  from the appropriate formula (A.1), (A.2) or (A.3), using the fit parameters from Tab. A or B;
- calculate  $f^{a_{1,2,4}}$  from (A.6), using the fit parameters from Tab. C;
- calculate the total formfactor from (A.5);
- extend the formfactor to the full kinematical regime by fitting it to (A.1), (A.2) or (A.3).



## B Distribution Amplitudes

In this appendix we collect explicit expressions for all the DAs that enter the formfactors. These expressions are well known and have been taken from Ref. [16].

The key point is that, to leading order in QCD, DAs can be expressed as a partial wave expansion in terms of contributions of increasing conformal spin, the so-called conformal expansion. The coefficients of different partial waves renormalize multiplicatively to LO in QCD, but mix at NLO, the reason being that the symmetry underlying the conformal expansion, the conformal symmetry of massless QCD, is anomalous and broken by radiative corrections.

The two-particle twist-2 amplitude (8) is expanded as

$$\phi(u, \mu) = \phi_{\text{as}}(u) \sum_{n \geq 0} a_n(\mu) C_n^{3/2}(\zeta) \quad (\text{A.8})$$

with  $\zeta \equiv 2u - 1$  and  $a_0 = 1$  from normalization:

$$\int_0^1 du \phi(u, \mu) = 1.$$

The  $C_n^{3/2}(\zeta)$  are Gegenbauer polynomials. The conformal spin of the term in  $C_n^{3/2}$  is  $j = n + 2$ . For the  $\pi$  and  $\eta$  one has  $a_{2n+1} = 0$  due to G-parity, but  $a_1^K \sim (m_s - m_q)$  for the  $K$  [33], which is one source of SU(3) breaking for the formfactors.

As only the first few Gegenbauer moments  $a_n$  are known numerically, we truncate the series at  $n = 4$ ; the values of the conformal spins included are listed in Tab. E, whereas the numerical values of the  $a_i$  are discussed in Sec. 4. The truncation is justified as long as the perturbative kernels  $T$  with which the DAs are convoluted are slowly varying functions of  $u$ , so that the rapidly oscillating Gegenbauers suppress terms with high  $n$ . In our case the  $T$  are nonsingular for all  $u$ , including the endpoints  $u = 0, 1$ , so the truncation of the series is justified. The term labeled  $\phi_{\text{as}}$  in (A.8) is the asymptotic DA which is reached for large scales  $\mu \rightarrow \infty$ ; it is completely determined by perturbation theory and given by

$$\phi_{\text{as}}(u) = 6u(1 - u);$$

it is the same for all mesons. The Gegenbauer moments  $a_n$  become relevant at moderate scales and depend on the hadron in question.

Let us now define the three-particle DAs. To twist-3 accuracy, there is only one:

$$\begin{aligned} \langle 0 | \bar{u}(x) \sigma_{\mu\nu} \gamma_5 g G_{\alpha\beta}(vx) d(-x) | \pi^-(p) \rangle &= \\ &= i \frac{f_\pi m_\pi^2}{m_u + m_d} (p_\alpha p_\mu g_{\nu\beta} - p_\alpha p_\nu g_{\mu\beta} - p_\beta p_\mu g_{\nu\alpha} + p_\beta p_\nu g_{\alpha\mu}) \mathcal{T}(v, p \cdot x) + \dots, \end{aligned} \quad (\text{A.9})$$

where the ellipses stand for Lorentz structures of twist-5 and higher and where we used the following short-hand notation for the integral defining the three particle DA:

$$\mathcal{T}(v, p \cdot x) = \int \mathcal{D}\underline{\alpha} e^{-ip \cdot x(\alpha_u - \alpha_d + v\alpha_g)} \mathcal{T}(\alpha_d, \alpha_u, \alpha_g). \quad (\text{A.10})$$

Here  $\underline{\alpha}$  is the set of three momentum fractions  $\alpha_d$  ( $d$  quark),  $\alpha_u$  ( $u$  quark) and  $\alpha_g$  (gluon). The integration measure is defined as

$$\int \mathcal{D}\underline{\alpha} = \int_0^1 d\alpha_d d\alpha_u d\alpha_g \delta(1 - \alpha_u - \alpha_d - \alpha_g).$$

There are also four three-particle DAs of twist-4, defined as

$$\begin{aligned} \langle 0 | \bar{u}(x) \gamma_\mu \gamma_5 g G_{\alpha\beta}(vx) d(-x) | \pi^-(p) \rangle &= \\ &= p_\mu (p_\alpha x_\beta - p_\beta x_\alpha) \frac{1}{p \cdot x} f_\pi m_\pi^2 \mathcal{A}_\parallel(v, p \cdot x) + (p_\beta g_{\alpha\mu}^\perp - p_\alpha g_{\beta\mu}^\perp) f_\pi m_\pi^2 \mathcal{A}_\perp(v, p \cdot x) \end{aligned} \quad (\text{A.11})$$

$$\begin{aligned} \langle 0 | \bar{u}(x) \gamma_\mu i g \tilde{G}_{\alpha\beta}(vx) d(-x) | \pi^-(p) \rangle &= \\ &= p_\mu (p_\alpha x_\beta - p_\beta x_\alpha) \frac{1}{p \cdot x} f_\pi m_\pi^2 \mathcal{V}_\parallel(v, p \cdot x) + (p_\beta g_{\alpha\mu}^\perp - p_\alpha g_{\beta\mu}^\perp) f_\pi m_\pi^2 \mathcal{V}_\perp(v, p \cdot x) \end{aligned} \quad (\text{A.12})$$

$g_{\mu\nu}^\perp$  is defined as

$$g_{\mu\nu}^\perp = g_{\mu\nu} - \frac{1}{p \cdot x} (p_\mu x_\nu + p_\nu x_\mu).$$

To next-to-leading conformal spin ( $j = 7/2, 9/2$ ), the twist-3 three-particle distribution amplitude  $\mathcal{T}$  is given by<sup>15</sup>

$$\mathcal{T}(\alpha_u, \alpha_d, \alpha_g) = 360 \eta_3 \alpha_u \alpha_d \alpha_g^2 \{1 + \omega_3 \frac{1}{2} (7\alpha_g - 3)\} \quad .$$

The two-particle twist-3 distribution amplitudes  $\phi_p$  and  $\phi_\sigma$  in Eqs. (9) and (10) depend on  $\mathcal{T}$  through the equations of motions [16],<sup>16</sup> which implies that their coefficients are not independent from each other. The expansion up to NNL order ( $j = 3/2, 7/2, 9/2$ ) reads<sup>17</sup>

$$\phi_p(u) = 1 + \{30\eta_3 - \frac{5}{2}\rho_\pi^2\} C_2^{1/2}(\zeta) + \{-3\eta_3\omega_3 - \frac{27}{20}\rho_\pi^2 - \frac{81}{10}\rho_\pi^2 a_2\} C_4^{1/2}(\zeta),$$

$$\phi_\sigma(u) = 6u(1-u) \{1 + \{5\eta_3 - \frac{1}{2}\eta_3\omega_3 - \frac{7}{20}\rho_\pi^2 - \frac{3}{5}\rho_\pi^2 a_2\} C_2^{3/2}(\zeta) \quad .$$

The two-particle twist-4 corrections  $g_\pi$  and  $\mathbb{A}$  in Eq. (8) are given to NNL conformal spin

<sup>15</sup>In the literature the notation  $f_{3\pi} = f_\pi \eta_3$  is also widely used.

<sup>16</sup>An explicit expression for  $\phi_p$  in terms of  $\mathcal{T}$  is given in Ref. [41], Eq. (16).

<sup>17</sup>At first glance it seems that  $\phi_p$  is taken to a higher order in conformal expansion than  $\phi_\sigma$ , but as discussed in the first reference of [16],  $\phi_p$  and  $\phi_\sigma$  are not pure spin projections, which means that the coefficients of a given Gegenbauer polynomial contain contributions from different partial waves.

( $j = 1, 3, 5$ ) by<sup>18</sup>

$$\begin{aligned}
g_\pi(u) &= 1 + \left\{1 + \frac{18}{7}a_2 + 60\eta_3 + \frac{20}{3}\eta_4\right\}C_2^{1/2}(\zeta) + \left\{-\frac{9}{28}a_2 - 6\eta_3\omega_3\right\}C_4^{1/2}(\zeta), \\
\mathbb{A}(u) &= 6u\bar{u} \left\{ \frac{16}{15} + \frac{24}{35}a_2 + 20\eta_3 + \frac{20}{9}\eta_4 \right. \\
&\quad + \left( -\frac{1}{15} + \frac{1}{16} - \frac{7}{27}\eta_3\omega_3 - \frac{10}{27}\eta_4 \right) C_2^{3/2}(\xi) + \left( -\frac{11}{210}a_2 - \frac{4}{135}\eta_3\omega_3 \right) C_4^{3/2}(\xi) \Big\} \\
&\quad + \left( -\frac{18}{5}a_2 + 21\eta_4\omega_4 \right) \left\{ 2u^3(10 - 15u + 6u^2) \ln u + 2\bar{u}^3(10 - 15\bar{u} + 6\bar{u}^2) \ln \bar{u} \right. \\
&\quad \left. + u\bar{u}(2 + 13u\bar{u}) \right\}.
\end{aligned}$$

Finally the three-particle twist-4 DAs are to NL spin ( $j = 3, 5$ ) given by

$$\begin{aligned}
\mathcal{A}_\parallel(\underline{\alpha}) &= 120\alpha_u\alpha_d\alpha_g(a_{10}(\alpha_d - \alpha_u)), \\
\mathcal{V}_\parallel(\underline{\alpha}) &= 120\alpha_u\alpha_d\alpha_g(v_{00} + v_{10}(3\alpha_g - 1)), \\
\mathcal{A}_\perp(\underline{\alpha}) &= 30\alpha_g^2(\alpha_u - \alpha_d)[h_{00} + h_{01}\alpha_g + h_{10}(5\alpha_g - 3)/2], \\
\mathcal{V}_\perp(\underline{\alpha}) &= -30\alpha_g^2\{h_{00}\bar{\alpha}_g + h_{01}[\alpha_g\bar{\alpha}_g - 6\alpha_u\alpha_d] + h_{10}[\alpha_g\bar{\alpha}_g - 3/2(\alpha_u^2 + \alpha_d^2)]\},
\end{aligned}$$

where  $\bar{\alpha} = 1 - \alpha$  and the  $a_{ij}$ ,  $v_{ij}$  and  $h_{ij}$  are related to hadronic matrix elements  $\eta_4$ ,  $\omega_4$  and  $a_2$  as

$$\begin{aligned}
a_{10} &= \frac{21}{8}\eta_4\omega_4 - \frac{9}{20}a_2, & v_{10} &= \frac{21}{8}\eta_4\omega_4, & v_{00} &= -\frac{1}{3}\eta_4, \\
h_{01} &= \frac{7}{4}\eta_4\omega_4 - \frac{3}{20}a_2, & h_{10} &= \frac{7}{2}\eta_4\omega_4 + \frac{3}{20}a_2, & v_{00} &= -\frac{1}{3}\eta_4.
\end{aligned}$$

Taking everything together, we have 7 hadronic parameters  $\{c_i\} = \{a_1, a_2, a_4, \eta_3, \omega_3, \eta_4, \omega_4\}$  which parametrize all DAs to twist-4 and NLO in conformal spin. The  $c_i$  are scale-dependent and are usually given at the scale 1 GeV. To LO in QCD, they do not mix under renormalisation, so that the scaling up to  $\mu_{\text{IR}} = \sqrt{m_B^2 - m_b^2}$  is given by

$$c_i(\mu_{\text{IR}}) = L^{\gamma_{c_i}/\beta_0} c_i(1 \text{ GeV}),$$

with  $L = \alpha_s(\mu_{\text{IR}})/\alpha_s(1 \text{ GeV})$ ,  $\beta_0 = 11 - 2/3N_f$ . The one-loop anomalous dimensions  $\gamma_{c_i}$  are given in Tab. F. Note that the anomalous dimension increases with increasing conformal spin,  $\gamma \sim \log j$ , which implies that the truncation of the conformal expansion becomes the better the high the scale. The numerical values for all these parameters at the scale  $\mu = 1 \text{ GeV}$  are collected in Tab. G, taken from Ref. [16].

---

<sup>18</sup>Note that, contrary to appearances, the contributions of  $g_\pi$  and  $\mathbb{A}$  to (8) do not vanish for zero meson mass:  $\eta_4$  implicitly contains a factor  $1/m_\pi^2$  and survives in the limit  $m_\pi^2 \rightarrow 0$ .

	tree					$O(\alpha_s)$				
twist	2	3		4		2	3		4	
x-particle	2	2	3	2	3	2	2	3	2	3
$j_L$	2	$\frac{3}{2}$	$\frac{7}{2}$	1	3	2	$\frac{3}{2}$	-	-	-
$j_{NL}$	4	$\frac{7}{2}$	$\frac{9}{2}$	3	5	4	$\frac{7}{2}$	-	-	-
$j_{NNL}$	6	$\frac{9}{2}$	-	5	-	6	-	-	-	-

Table E: Overview of the contributions included in the calculations. For the  $K$  we also include conformal spin  $j = 3$  for twist-2 which explicitly parametrizes SU(3) flavor breaking.

$\gamma_{a_n}$	$\gamma_{\eta_3}$	$\gamma_{\omega_3}$	$\gamma_{\eta_4}$	$\gamma_{\omega_4}$
$C_F \left( 1 - \frac{2}{(n+1)(n+2)} - \sum_{m=2}^{n+1} \frac{1}{m} \right)$	$\frac{16}{3}C_F + C_A$	$-\frac{25}{6}C_F + \frac{7}{3}C_A$	$\frac{8}{3}C_F$	$-\frac{8}{3}C_F + \frac{10}{3}C_A$

Table F: One-loop anomalous dimensions of hadronic parameters in DAs.

	$\pi$	$K$	$\eta$
$\eta_3$	0.015	0.015	0.013
$\omega_3$	-3	-3	-3
$\eta_4$	10	0.6	0.5
$\omega_4$	0.2	0.2	0.2

Table G: Input parameters for twist-3 and 4 DAs, calculated from QCD sum rules. The accuracy is about 50%. Renormalization scale is 1 GeV.

## C Spectral Densities for $f_+$

The total spectral density of  $\Pi_+$  is obtained as sum of all the contributions listed below, i.e.

$$\rho_{\Pi_+} = \rho_{T2} + \rho_{T3} + \rho_\sigma + \rho_p + \rho_{T4}^{2p} + \rho_{T4}^{3p}.$$

$\rho_{T2}$  is the contribution from the twist-2 DA,  $\rho_{T3}$  from the twist-3 three-particle DA,  $\rho_{\sigma(p)}$  from the twist-3 two-particle DA  $\phi_{\sigma(p)}$  and  $\rho_{T4}^{2(3)p}$  from the two(three)-particle DAs of twist-4. There is also one constant term,  $T4_c$ , which is due to twist-4 corrections that cannot be expressed via a dispersion relation, so that the total Borel-transformed  $\Pi_+$  is given as

$$\hat{B}\Pi_+ = \int_{m_b^2}^{\infty} ds \rho_{\Pi_+}(s) e^{-s/M^2} + T4_c.$$

$$\begin{aligned}
\rho_{T2} = & \frac{3 f_{\pi} m_b}{(q^2 - s)^7} (m_b^2 - q^2) (m_b^2 - s) (15 a_4 (42 m_b^8 + q^8 + 10 q^6 s + 20 q^4 s^2 + 10 q^2 s^3 + s^4 \\
& - 84 m_b^6 (q^2 + s) + 28 m_b^4 (2 q^2 + s) (q^2 + 2 s) - 14 m_b^2 (q^2 + s) (q^4 + 4 q^2 s + s^2)) + (q^2 - s)^2 \\
& \times (6 a_2 (5 m_b^4 + q^4 + 3 q^2 s + s^2 - 5 m_b^2 (q^2 + s)) + (q^2 - s) (a_0 (q^2 - s) + 3 a_1 (-2 m_b^2 + q^2 + s)))) \\
& + \mathbf{a}_s \left\{ \frac{3 \mathbf{a}_0 f_{\pi} m_b}{s(q^2 - s)^3} ((m_b^2 - s) (-2 m_b^2 q^2 + 2 q^4 + m_b^2 (4 + \pi^2) s - (1 + \pi^2) q^2 s - 3 s^2) + (m_b^2 - q^2) \right. \\
& \times (s (s - m_b^2) \log(1 - \frac{q^2}{m_b^2})^2 + s \log(\frac{s}{m_b^2}) (-2 s + (m_b^2 - s) \log(\frac{s}{m_b^2})) + 2 (m_b^2 - s) (2 m_b^2 - 5 s \\
& + 2 s \log(\frac{s}{m_b^2})) \log(\frac{s}{m_b^2} - 1) + 2 s (s - m_b^2) \log(\frac{s}{m_b^2} - 1)^2 - 2 (m_b^2 - s) \log(1 - \frac{q^2}{m_b^2}) (m_b^2 \\
& + s + s \log(\frac{s}{m_b^2}) - 2 s \log(\frac{s}{m_b^2} - 1))) + 2 (m_b^2 - q^2) (m_b^2 - s) (\text{Li}_2(\frac{q^2}{q^2 - m_b^2}) + \text{Li}_2(1 - \frac{m_b^2}{s} \\
& + 4 \text{Li}_2(1 - \frac{s}{m_b^2}))) + \frac{\mathbf{a}_1 f_{\pi} m_b}{s(q^2 - s)^4} ((m_b^2 - s) (6 q^2 (6 m_b^4 - 6 m_b^2 q^2 + q^4) + (-2 m_b^4 (95 + 9 \pi^2) \\
& + 27 m_b^2 (6 + \pi^2) q^2 + (3 - 9 \pi^2) q^4) s + (m_b^2 (158 + 9 \pi^2) - 3 (50 + 3 \pi^2) q^2) s^2 - 13 s^3) + 3 (8 (m_b^2 - s) \\
& \times (q^2 - m_b^2) (2 m_b^2 - q^2 - s) s \log(\frac{\mu^2}{m_b^2}) + 3 (m_b^2 - q^2) (m_b^2 - s) (2 m_b^2 - q^2 - s) s \log(1 - \frac{q^2}{m_b^2})^2 \\
& + s \log(\frac{s}{m_b^2}) (12 m_b^4 (q^2 + s) + 14 q^2 s (q^2 + s) - 2 m_b^2 (4 q^4 + 19 q^2 s + 7 s^2) - 3 (m_b^2 - q^2) (m_b^2 - s) \\
& \times (2 m_b^2 - q^2 - s) \log(\frac{s}{m_b^2})) - 2 (m_b^2 - q^2) (s - m_b^2) (-2 m_b^2 + q^2 + s) (6 m_b^2 - 23 s + 6 s \log(\frac{s}{m_b^2})) \\
& \times \log(\frac{s}{m_b^2} - 1) + 6 (m_b^2 - q^2) s (s - m_b^2) (-2 m_b^2 + q^2 + s) \log(\frac{s}{m_b^2} - 1)^2 + 6 (m_b^2 - q^2) \\
& \times (m_b^2 - s) (2 m_b^2 - q^2 - s) \log(1 - \frac{q^2}{m_b^2}) (m_b^2 - s + s \log(\frac{s}{m_b^2}) - 2 s \log(\frac{s}{m_b^2} - 1))) - 18 (m_b^2 - q^2) \\
& \times (m_b^2 - s) (2 m_b^2 - q^2 - s) (\text{Li}_2(\frac{q^2}{q^2 - m_b^2}) + \text{Li}_2(1 - \frac{m_b^2}{s}) + 4 \text{Li}_2(1 - \frac{s}{m_b^2}))) \\
& + \frac{\mathbf{a}_2 f_{\pi} m_b}{4 s(q^2 - s)^5} ((m_b^2 - s) (-24 (m_b^2 - q^2) q^2 (30 m_b^4 - 15 m_b^2 q^2 + q^4) + (5 m_b^6 (1183 + 72 \pi^2) \\
& - 20 m_b^4 (407 + 36 \pi^2) q^2 + 12 (5 - 6 \pi^2) q^6 + 216 m_b^2 (11 + 2 \pi^2) q^4) s - (5 m_b^4 (1525 + 72 \pi^2) \\
& - 16 m_b^2 (575 + 36 \pi^2) q^2 + 36 (73 + 6 \pi^2) q^4) s^2 + (m_b^2 (2083 + 72 \pi^2) - 8 (260 + 9 \pi^2) q^2) s^3 - 61 s^4)
\end{aligned}$$

$$\begin{aligned}
& + 12 (25 (m_b^2 - q^2) (m_b^2 - s) s (5 m_b^4 + q^4 + 3 q^2 s + s^2 - 5 m_b^2 (q^2 + s)) \log(\frac{\mu^2}{m_b^2}) - 6 (m_b^2 - q^2) \\
& \times (m_b^2 - s) s (5 m_b^4 + q^4 + 3 q^2 s + s^2 - 5 m_b^2 (q^2 + s)) \log(1 - \frac{q^2}{m_b^2})^2 + s \log(\frac{s}{m_b^2}) (-60 m_b^6 (q^2 + s) \\
& + 37 q^2 s (q^4 + 3 q^2 s + s^2) + 30 m_b^4 (3 q^4 + 8 q^2 s + 3 s^2) - m_b^2 (25 q^6 + 237 q^4 s + 261 q^2 s^2 + 37 s^3) \\
& + 6 (m_b^2 - q^2) (m_b^2 - s) (5 m_b^4 + q^4 + 3 q^2 s + s^2 - 5 m_b^2 (q^2 + s)) \log(\frac{s}{m_b^2})) + 2 (m_b^2 - q^2) (m_b^2 - s) \\
& \times (5 m_b^4 + q^4 + 3 q^2 s + s^2 - 5 m_b^2 (q^2 + s)) (12 m_b^2 - 55 s + 12 s \log(\frac{s}{m_b^2})) \log(\frac{s}{m_b^2} - 1) + 12 s \\
& \times (m_b^2 - q^2) (s - m_b^2) (5 m_b^4 + q^4 + 3 q^2 s + s^2 - 5 m_b^2 (q^2 + s)) \log(\frac{s}{m_b^2} - 1)^2 - 12 (m_b^2 - q^2) \\
& \times (m_b^2 - s) (5 m_b^4 + q^4 + 3 q^2 s + s^2 - 5 m_b^2 (q^2 + s)) \log(1 - \frac{q^2}{m_b^2}) (m_b^2 - s + s \log(\frac{s}{m_b^2}) - 2 s \\
& \times \log(\frac{s}{m_b^2} - 1))) + 144 (m_b^2 - q^2) (m_b^2 - s) (5 m_b^4 + q^4 + 3 q^2 s + s^2 - 5 m_b^2 (q^2 + s)) \\
& \times (\text{Li}_2(\frac{q^2}{q^2 - m_b^2}) + \text{Li}_2(1 - \frac{m_b^2}{s}) + 4 \text{Li}_2(1 - \frac{s}{m_b^2}))) \\
& + \frac{\mathbf{a}_4 f_\pi m_b}{10 s (q^2 - s)^7} (-(m_b^2 - s) (30 (m_b^2 - q^2) q^2 (1260 m_b^8 - 1890 m_b^6 q^2 - 105 m_b^2 q^6 + 2 q^8 \\
& + 840 m_b^4 q^4) - (21 m_b^{10} (23207 + 900 \pi^2) - 63 m_b^8 (18827 + 900 \pi^2) q^2 - 700 m_b^4 (439 + 45 \pi^2) q^6 \\
& + 150 m_b^2 (176 + 45 \pi^2) q^8 + 30 (19 - 15 \pi^2) q^{10} + 175 m_b^6 (5603 + 360 \pi^2) q^4) s + 84 (m_b^8 \\
& \times (13051 + 450 \pi^2) - 112 m_b^6 (22157 + 900 \pi^2) q^2 - 800 m_b^2 (616 + 45 \pi^2) q^6 + 150 (283 + 30 \pi^2) q^8 \\
& + 525 m_b^4 (3523 + 180 \pi^2) q^4) s^2 (-7 m_b^6 (119363 + 3600 \pi^2) + 756 m_b^4 (2131 + 75 \pi^2) q^2 + 200 (848 \\
& + 45 \pi^2) q^6 - 10125 m_b^2 (89 + 4 \pi^2) q^4) s^3 + (7 m_b^4 (34967 + 900 \pi^2) - 6 m_b^2 (57989 + 1800 \pi^2) q^2 \\
& + 125 (1075 + 36 \pi^2) q^4) s^4 + (-2 m_b^2 (10553 + 225 \pi^2) + (21461 + 450 \pi^2) q^2) s^5 + 181 s^6)) + 30 \\
& \times (91 (m_b^2 - q^2) (m_b^2 - s) s (42 m_b^8 + q^8 + 10 q^6 s + 20 q^4 s^2 + 10 q^2 s^3 + s^4 - 84 m_b^6 (q^2 + s) \\
& + 28 m_b^4 (2 q^2 + s) (q^2 + 2 s) - 14 m_b^2 (q^2 + s) (q^4 + 4 q^2 s + s^2)) \log(\frac{\mu^2}{m_b^2}) - 15 (m_b^2 - q^2) (m_b^2 - s) s \\
& \times (42 m_b^8 + q^8 + 10 q^6 s + 20 q^4 s^2 + 10 q^2 s^3 + s^4 - 84 m_b^6 (q^2 + s) + 28 m_b^4 (2 q^2 + s) (q^2 + 2 s) - 14 m_b^2 \\
& \times (q^2 + s) (q^4 + 4 q^2 s + s^2)) \log(1 - \frac{q^2}{m_b^2})^2 + s \log(\frac{s}{m_b^2}) (-1260 m_b^{10} (q^2 + s) + 630 m_b^8 (5 q^4
\end{aligned}$$

$$\begin{aligned}
& + 12 q^2 s + 5 s^2) - 210 m_b^6 (q^2 + s) (13 q^4 + 48 q^2 s + 13 s^2) + 121 q^2 s (q^8 + 10 q^6 s + 20 q^4 s^2 \\
& + 10 q^2 s^3 + s^4) + 105 m_b^4 (9 q^8 + 82 q^6 s + 160 q^4 s^2 + 82 q^2 s^3 + 9 s^4) - m_b^2 (91 q^{10} \\
& + 2305 q^8 s + 9400 q^6 s^2 + 9700 q^4 s^3 + 2575 q^2 s^4 + 121 s^5) + 15 (m_b^2 - q^2) (m_b^2 - s) \\
& \times (42 m_b^8 + q^8 + 10 q^6 s + 20 q^4 s^2 + 10 q^2 s^3 + s^4 - 84 m_b^6 (q^2 + s) + 28 m_b^4 (2 q^2 + s) (q^2 + 2 s) \\
& - 14 m_b^2 (q^2 + s) (q^4 + 4 q^2 s + s^2)) \log\left(\frac{s}{m_b^2}\right) + 4 (m_b^2 - q^2) (m_b^2 - s) (42 m_b^8 + q^8 + 10 q^6 s \\
& + 20 q^4 s^2 + 10 q^2 s^3 + s^4 - 84 m_b^6 (q^2 + s) + 28 m_b^4 (2 q^2 + s) (q^2 + 2 s) - 14 m_b^2 (q^2 + s) \\
& \times (q^4 + 4 q^2 s + s^2)) (15 m_b^2 - 83 s + 15 s \log\left(\frac{s}{m_b^2}\right)) \log\left(\frac{s}{m_b^2} - 1\right) + 30 (m_b^2 - q^2) s (s - m_b^2) \\
& \times (42 m_b^8 + q^8 + 10 q^6 s + 20 q^4 s^2 + 10 q^2 s^3 + s^4 - 84 m_b^6 (q^2 + s) + 28 m_b^4 (2 q^2 + s) (q^2 + 2 s) \\
& - 14 m_b^2 (q^2 + s) (q^4 + 4 q^2 s + s^2)) \log\left(\frac{s}{m_b^2} - 1\right)^2 - 30 (m_b^2 - q^2) (m_b^2 - s) (42 m_b^8 + q^8 \\
& + 10 q^6 s + 20 q^4 s^2 + 10 q^2 s^3 + s^4 - 84 m_b^6 (q^2 + s) + 28 m_b^4 (2 q^2 + s) (q^2 + 2 s) - 14 m_b^2 \\
& \times (q^2 + s) (q^4 + 4 q^2 s + s^2)) \log\left(1 - \frac{q^2}{m_b^2}\right) (m_b^2 - s + s \log\left(\frac{s}{m_b^2}\right) - 2 s \log\left(\frac{s}{m_b^2} - 1\right)) \\
& + 900 s (m_b^2 - q^2) (m_b^2 - s) (42 m_b^8 + q^8 + 10 q^6 s + 20 q^4 s^2 + 10 q^2 s^3 + s^4 - 84 m_b^6 (q^2 + s) \\
& + 28 m_b^4 (2 q^2 + s) (q^2 + 2 s) - 14 m_b^2 (q^2 + s) (q^4 + 4 q^2 s + s^2)) \left(\text{Li}_2\left(\frac{q^2}{q^2 - m_b^2}\right) + \text{Li}_2\left(1 - \frac{m_b^2}{s}\right)\right. \\
& \left. + 4 \text{Li}_2\left(1 - \frac{s}{m_b^2}\right)\right)\} \\
\rho_{\text{T3}} = & \frac{-15 \eta_3 \mu_\pi^2}{(q^2 - s)^6} (m_b^2 - q^2)^2 (m_b^2 - s) (2 (q^2 - s) (-5 m_b^2 + 2 q^2 + 3 s) + (7 m_b^4 - 6 m_b^2 q^2 + q^4 - 8 m_b^2 s \\
& + 4 q^2 s + 2 s^2) \omega_3)
\end{aligned}$$



$$\begin{aligned}
\rho_P = & \frac{a_0 \mu_\pi^2 (3 m_b^2 s - 3 q^2 s)}{6 (q^2 - s)^2 s} + \frac{5 \eta_3 \mu_\pi^2}{(q^2 - s)^4 s} (18 m_b^6 s - 36 m_b^4 q^2 s - 3 q^6 s + 21 m_b^2 q^4 s - 18 m_b^4 s^2 \\
& + 30 m_b^2 q^2 s^2 - 12 q^4 s^2 + 3 m_b^2 s^3 - 3 q^2 s^3) + \mathbf{a}_s \left\{ \frac{\mathbf{a}_0 \mu_\pi^2}{6 (q^2 - s)^2 s} ((q^2 + s) (s - 3 m_b^2) \right. \\
& - 3 (m_b^2 - 4 q^2) s \log\left(\frac{q^2}{m_b^2}\right)^2 - 18 s (3 m_b^2 - 3 q^2 + s) \log\left(1 - \frac{q^2}{m_b^2}\right)^2 (m_b^2 - 4 q^2) s \log\left(\frac{q^2}{m_b^2}\right) \\
& \times (\log(1 - \frac{q^2}{m_b^2}) - \log(\frac{s - q^2}{m_b^2})) + 6 \log(1 - \frac{q^2}{m_b^2}) (m_b^2 q^2 + 3 m_b^2 s - q^2 s + s ((2 m_b^2 - 3 q^2) \\
& \times \log(\frac{\mu^2}{m_b^2}) + q^2 \log(\frac{s}{m_b^2}) (m_b^2 + q^2 + s) \log(\frac{s - q^2}{m_b^2}) - (m_b^2 - 2 q^2) \log(\frac{s}{m_b^2} - 1))) + 3 (m_b^2 s \\
& \times \log(\frac{s}{m_b^2})^2 - \log(\frac{s - q^2}{m_b^2}) s (5 q^2 + s) + \log(\frac{s}{m_b^2}) (2 m_b^2 q^2 + m_b^2 s - 3 q^2 s - 4 q^2 s \log(\frac{s}{m_b^2} - 1)) \\
& + 2 \log(\frac{s - q^2}{m_b^2}) (2 q^2 s - m_b^2 (q^2 + s) - s (2 m_b^2 - 3 q^2 + s) \log(\frac{\mu^2}{m_b^2}) + s (3 m_b^2 - 2 q^2 + 2 s) \\
& \times \log(\frac{s}{m_b^2} - 1)) + 2 \log(\frac{s}{m_b^2} - 1) (2 q^2 s - m_b^2 (q^2 + 4 s) + s (s \log(\frac{\mu^2}{m_b^2}) - (m_b^2 + 2 s) \log(\frac{s}{m_b^2} - 1))) \\
& + 6 s (m_b^2 \text{Li}_2(\frac{q^2}{q^2 - m_b^2}) + (2 m_b^2 - 3 q^2 + s) \text{Li}_2(1 - \frac{q^2}{m_b^2}) + m_b^2 \text{Li}_2(1 - \frac{m_b^2}{s}) - (m_b^2 + q^2 + s) \\
& \times \text{Li}_2(1 - \frac{q^2}{s}) - (5 q^2 + s) \text{Li}_2(\frac{m_b^2 - s}{m_b^2 - q^2}) - (m_b^2 + q^2 + s) \text{Li}_2(\frac{m_b^2 - s}{q^2 - s}) - (m_b^2 + q^2 + s) \\
& \times \text{Li}_2(\frac{(q^2 - m_b^2) s}{m_b^2 (q^2 - s)}) + (2 m_b^2 - 3 q^2 + s) \text{Li}_2(\frac{m_b^2 - q^2}{s - q^2}) + 2 (m_b^2 - q^2) \text{Li}_2(1 - \frac{s}{m_b^2}) + (m_b^2 - 4 q^2) \\
& \times \text{Li}_2(1 - \frac{s}{q^2})) 6 (q^2 - s)^2 s + \frac{5 \eta_3 \mu_\pi^2}{(q^2 - s)^4 s} (-3 m_b^2 (q^2 - 12 m_b^2) q^4 - 6 m_b^6 (\pi^2 - 47) s - 18 m_b^4 (24 \\
& + \pi^2) q^2 s + (3 + 2 \pi^2) q^6 s + 3 m_b^2 (8 \pi^2 - 17) q^4 s + 6 m_b^4 (\pi^2 - 60) s^2 + 3 m_b^2 (205 + 6 \pi^2) q^2 s^2 \\
& - (3 + 26 \pi^2) q^4 s^2 + 69 m_b^2 s^3 - (147 + 2 \pi^2) q^2 s^3 + (-9 + 2 \pi^2) s^4 + 3 (m_b^2 - 4 q^2) (q^2 - s)^2 s \log(\frac{q^2}{m_b^2})^2 \\
& + 6 (m_b^2 - 4 q^2) (q^2 - s)^2 s \log(\frac{q^2}{m_b^2}) (\log(1 - \frac{q^2}{m_b^2}) - \log(\frac{s - q^2}{m_b^2})) + 6 s \log(\frac{\mu^2}{m_b^2}) (15 m_b^6 - 15 m_b^4 (2 q^2 + s) \\
& - 3 q^2 s (q^2 + 4 s) + m_b^2 (9 q^4 + 30 q^2 s + 6 s^2) + (6 m_b^6 - 6 m_b^4 s - 3 q^2 (q^4 - 4 q^2 s + s^2) + m_b^2 (-4 q^4 - 4 q^2 s)
\end{aligned}$$

$$\begin{aligned}
& + 2 s^2)) \log(1 - \frac{q^2}{m_b^2}) - (q^2 - s)^2 (2 m_b^2 - 3 q^2 + s) \log(\frac{s - q^2}{m_b^2}) + (-6 m_b^6 + 6 m_b^2 q^4 + 6 m_b^4 s + s (-5 q^4 \\
& - 2 q^2 s + s^2)) \log(\frac{s}{m_b^2} - 1)) + 3 (-s (6 m_b^6 - (q^2 - s)^2 (3 q^2 - s) - 6 m_b^4 (q^2 + s) + 3 m_b^2 (q^4 + s^2)) \\
& - \log(1 - \frac{q^2}{m_b^2})^2 + m_b^2 s (6 m_b^4 + q^4 + 4 q^2 s + s^2 6 m_b^2 (q^2 + s)) \log(\frac{s}{m_b^2})^2 - (q^2 - s)^2 \log(\frac{s - q^2}{m_b^2}) \\
& \times (2 (-2 q^2 s + m_b^2 (q^2 + s)) + s (5 q^2 + s) \log(\frac{s - q^2}{m_b^2})) 2 (6 m_b^6 (2 q^2 + 9 s) - 6 m_b^4 (2 q^4 + 18 q^2 s + 9 s^2) \\
& - 2 q^2 s (q^4 + 7 q^2 s + 13 s^2) + m_b^2 (q^6 + 44 q^4 s + 89 q^2 s^2 + 16 s^3) (-3 m_b^2 + 2 q^2 - 2 s) (q^2 - s)^2 s \\
& \times \log(\frac{s - q^2}{m_b^2})) \log(\frac{s}{m_b^2} - 1) - 2 s (-6 m_b^6 - 6 m_b^4 (q^2 - s) + 2 s (-5 q^4 - 2 q^2 s + s^2) m_b^2 (13 q^4 + 4 q^2 s \\
& + s^2)) \log(\frac{s}{m_b^2} - 1)^2 + \log(\frac{s}{m_b^2}) (-12 m_b^4 s^2 - 3 q^2 s (q^2 + 3 s)^2 + m_b^2 (2 q^6 + 21 q^4 s + 12 q^2 s^2 + 13 s^3) \\
& - 4 q^2 s (6 m_b^4 + q^4 + 4 q^2 s + s^2 - 6 m_b^2 (q^2 + s)) \log(\frac{s}{m_b^2} - 1)) + 2 \log(1 - \frac{q^2}{m_b^2}) (6 m_b^6 (q^2 + 2 s) \\
& - q^2 s (q^4 - 8 q^2 s + s^2) - 6 m_b^4 (q^4 + 2 q^2 s + 2 s^2) + m_b^2 (q^6 + q^4 s + q^2 s^2 + 3 s^3) + s (q^2 (6 m_b^4 + q^4 \\
& + 4 q^2 s + s^2 - 6 m_b^2 (q^2 + s)) \log(\frac{s}{m_b^2}) + (q^2 - s)^2 (m_b^2 + q^2 + s) \log(\frac{s - q^2}{m_b^2}) + (-12 m_b^4 q^2 + m_b^2 (11 q^4 \\
& + 14 q^2 s - s^2) + 2 q^2 (q^4 - 8 q^2 s + s^2)) \log(\frac{s}{m_b^2} - 1))) + 6 s (m_b^2 (6 m_b^4 + q^4 + 4 q^2 s + s^2 - 6 m_b^2 \\
& \times (q^2 + s)) \text{Li}_2(\frac{q^2}{q^2 - m_b^2}) + (q^2 - s)^2 (2 m_b^2 - 3 q^2 + s) \text{Li}_2(1 - \frac{q^2}{m_b^2}) + m_b^2 (6 m_b^4 + q^4 + 4 q^2 s + s^2 \\
& - 6 m_b^2 (q^2 + s)) \text{Li}_2(1 - \frac{m_b^2}{s}) (q^2 - s)^2 (m_b^2 + q^2 + s) \text{Li}_2(1 - \frac{q^2}{s}) - (q^2 - s)^2 (5 q^2 + s) \text{Li}_2(\frac{m_b^2 - s}{m_b^2 - q^2}) \\
& - (q^2 - s)^2 (m_b^2 + q^2 + s) \text{Li}_2(\frac{m_b^2 - s}{q^2 - s}) - (q^2 - s)^2 (m_b^2 + q^2 + s) \text{Li}_2(\frac{(q^2 - m_b^2) s}{m_b^2 (q^2 - s)}) + (q^2 - s)^2 (2 m_b^2 \\
& - 3 q^2 + s) \text{Li}_2(\frac{m_b^2 - q^2}{s - q^2}) + 2 (m_b^2 - q^2) (6 m_b^4 + q^4 + 4 q^2 s + s^2 - 6 m_b^2 (q^2 + s)) \text{Li}_2(1 - \frac{s}{m_b^2}) + (m_b^2 \\
& - 4 q^2) (q^2 - s)^2 \text{Li}_2(1 - \frac{s}{q^2})) \}
\end{aligned}$$

$$\begin{aligned}
\rho_\sigma = & \frac{\mu_\pi^2}{2(q^2 - s)^5} (a_0 (q^2 - s)^2 (-(m_b^2 (3q^2 + s)) + q^2 (q^2 + 3s)) - 30\eta_3 (10m_b^8 + 10m_b^6 (q^2 - s) \\
& - 30m_b^4 q^2 (q^2 + s) + m_b^2 (13q^6 + 45q^4 s + 21q^2 s^2 + s^3) - q^2 (q^6 + 11q^4 s + 15q^2 s^2 + 3s^3))) \\
& + \mathbf{a}_s \left\{ \frac{\mathbf{a}_0 \mu_\pi^2}{6(q^2 - s)^3 s} (3m_b^2 q^4 + q^2 (-4m_b^2 (-9 + \pi^2) + (-3 + 2\pi^2) q^2) s + (m_b^2 (21 - 4\pi^2) \right. \\
& + 4(-15 + \pi^2) q^2) s^2 + (3 + 2\pi^2) s^3 + 6s (-4q^2 s + m_b^2 (3q^2 + s)) \log(1 - \frac{q^2}{m_b^2})^2 + 6s \log(\frac{\mu^2}{m_b^2}) \\
& \times (3(-2q^2 s + m_b^2 (q^2 + s)) + (q^2 - s) (-(m_b^2 + q^2) \log(1 - \frac{q^2}{m_b^2})) - (m_b^2 + q^2 + s) \log(\frac{m_b^2 - s}{q^2 - s}) \\
& - (m_b^2 - 4q^2) \log(\frac{m_b^2 - q^2}{s - q^2}) + (m_b^2 + q^2) \log(\frac{s}{m_b^2} - 1))) + 3(-2(q^2 - s) s (m_b^2 + q^2 + s) \log(\frac{s}{m_b^2})^2 \\
& + 2(q^2 - s) \log(\frac{m_b^2 - s}{q^2 - s}) (- (m_b^2 (q^2 + 2s)) + s (m_b^2 + q^2 + s) \log(\frac{s - q^2}{m_b^2})) + (q^2 - s) s ((m_b^2 \\
& + q^2 + s) \log(\frac{m_b^2 - q^2}{s - q^2})^2 - (m_b^2 + q^2 + s) \log(\frac{(m_b^2 - q^2) s}{m_b^2 (s - q^2)})^2 - 2(m_b^2 + q^2 + s) \log(\frac{(m_b^2 - q^2) s}{m_b^2 (s - q^2)}) \\
& \times \log(\frac{s - q^2}{m_b^2}) + 2(2m_b^2 - 3q^2 + s) \log(\frac{s - q^2}{m_b^2})^2 + 2 \log(\frac{m_b^2 - q^2}{s - q^2}) (-3m_b^2 + 6q^2 + (2m_b^2 \\
& - 3q^2 + s) \log(\frac{s - q^2}{m_b^2}))) - 2(4m_b^4 (q^2 + s) + 2q^2 s (q^2 + 3s) - 2m_b^2 q^2 (q^2 + 7s) + (q^2 - s) s \\
& \times (5m_b^2 - 5q^2 + 3s) \log(\frac{s - q^2}{m_b^2})) \log(\frac{s}{m_b^2} - 1) + 2s (-2s (q^2 + s) + m_b^2 (3q^2 + s)) \log(\frac{s}{m_b^2} - 1)^2 \\
& + \log(\frac{s}{m_b^2}) (q^2 s (3q^2 + s) - m_b^2 (q^2 - s) (2q^2 + 5s) - 2(q^2 - s) s (m_b^2 + q^2 + s) (\log(\frac{m_b^2 - q^2}{s - q^2}) \\
& - \log(\frac{(m_b^2 - q^2) s}{m_b^2 (s - q^2)}) - \log(\frac{s - q^2}{m_b^2})) + 2s (-5m_b^2 q^2 + q^4 - 3m_b^2 s + 6q^2 s + s^2) \log(\frac{s}{m_b^2} - 1))) \\
& + 6 \log(1 - \frac{q^2}{m_b^2}) (- (q^2 (q^2 - 7s) s) + 2m_b^4 (q^2 + 2s) - m_b^2 (q^4 + 9q^2 s + 2s^2) + s ((4q^2 s - m_b^2 (3q^2 \\
& + s)) \log(\frac{q^2}{m_b^2}) + (2m_b^2 (q^2 + s) - q^2 (q^2 + 3s)) \log(\frac{s}{m_b^2}) + (q^2 - s) (-(m_b^2 + q^2 + s) (\log(\frac{m_b^2 - q^2}{s - q^2}) \\
& - \log(\frac{(m_b^2 - q^2) s}{m_b^2 (s - q^2)}))) - (m_b^2 - 4q^2) \log(\frac{s - q^2}{m_b^2})) - 2(q^2 (3q^2 - 7s) + m_b^2 (q^2 + 3s)) \log(\frac{s}{m_b^2} - 1))) \\
& + 6s ((4q^2 s - m_b^2 (3q^2 + s)) \text{Li}_2(1 - \frac{q^2}{m_b^2}) - (m_b^2 - 4q^2) (q^2 - s) (2 \text{Li}_2(\frac{m_b^2 - s}{m_b^2 - q^2}) + \text{Li}_2(\frac{m_b^2 - s}{q^2 - s})
\end{aligned}$$

$$\begin{aligned}
& -\text{Li}_2\left(\frac{q^2(m_b^2-s)}{m_b^2(q^2-s)}\right)) - (3m_b^2(3q^2+s) - (q^2+s)(5q^2+s))\text{Li}_2\left(1 - \frac{s}{m_b^2}\right)) + \frac{5\eta_3\mu_\pi^2}{6(q^2-s)^5s}(18m_b^2q^4 \\
& \times (40m_b^4 - 40m_b^2q^2 + q^4) + (5m_b^8(-359+24\pi^2) - 30m_b^6(127+16\pi^2)q^2 + 30m_b^4(129+20\pi^2)q^4 \\
& + 24m_b^2(40-11\pi^2)q^6 + 6(-3+2\pi^2)q^8)s + 2(5m_b^6(295-36\pi^2) + 30m_b^4(129+16\pi^2)q^2 - 6m_b^2 \\
& \times (609+68\pi^2)q^4 + 6(-27+20\pi^2)q^6)s^2 + 6(5m_b^4(-25+8\pi^2) - 19m_b^2(39+4\pi^2)q^2 + 9(55 \\
& + 4\pi^2)q^4)s^3 - 4(m_b^2(71+6\pi^2) - 66q^2)s^4 + (-37+12\pi^2)s^5 + 36s(10m_b^8 - 10m_b^6s - 10m_b^4q^2 \\
& \times (q^2+2s) - 4q^2s(q^4+3q^2s+s^2) + m_b^2(3q^6+25q^4s+21q^2s^2+s^3))\log\left(1 - \frac{q^2}{m_b^2}\right)^2 + 12s \\
& \times \log\left(\frac{\mu^2}{m_b^2}\right)(-(m_b^2(5m_b^2-2q^2)(5m_b^4+20m_b^2q^2-28q^4)) + (40m_b^6+135m_b^4q^2-249m_b^2q^4+47q^6)s \\
& - 3(5m_b^4+18m_b^2q^2-32q^4)s^2 + 9(m_b^2-2q^2)s^3 - 3(10m_b^8-20m_b^6(q^2+s)+10m_b^4(q^2+s) \\
& \times (2q^2+s) + q^2(q^6+7q^4s+3q^2s^2-s^3) - m_b^2(9q^6+23q^4s+7q^2s^2+s^3))\log\left(1 - \frac{q^2}{m_b^2}\right) \\
& + 3(q^2-s)^3(-(m_b^2+q^2+s)\log\left(\frac{m_b^2-s}{q^2-s}\right)) - (m_b^2-4q^2)\log\left(\frac{m_b^2-q^2}{s-q^2}\right)) + 3(10m_b^8-20m_b^6(q^2+s) \\
& + 10m_b^4(q^2+s)(2q^2+s) + q^2(q^6+7q^4s+3q^2s^2-s^3) - m_b^2(9q^6+23q^4s+7q^2s^2+s^3)) \\
& \times \log\left(\frac{s}{m_b^2}-1\right) + 36\log\left(1 - \frac{q^2}{m_b^2}\right)(20m_b^8q^2-10m_b^6q^2(3q^2+5s) + 2m_b^4(q^2+2s)(6q^4+13q^2s \\
& + s^2) - q^2s(q^6+q^4s-15q^2s^2-7s^3) - m_b^2(q^8+7q^6s+35q^4s^2+35q^2s^3+2s^4) + s((-10m_b^8 \\
& + 10m_b^6s+10m_b^4q^2(q^2+2s) + 4q^2s(q^4+3q^2s+s^2) - m_b^2(3q^6+25q^4s+21q^2s^2+s^3))\log\left(\frac{q^2}{m_b^2}\right) \\
& + (10m_b^6(2q^2+s) - 10m_b^4(3q^4+5q^2s+s^2) + 2m_b^2(6q^6+24q^4s+14q^2s^2+s^3) - q^2(q^6+11q^4s \\
& + 15q^2s^2+3s^3))\log\left(\frac{s}{m_b^2}\right) + (q^2-s)^3(-(m_b^2+q^2+s)(\log\left(\frac{m_b^2-q^2}{s-q^2}\right) - \log\left(\frac{(m_b^2-q^2)s}{m_b^2(s-q^2)}\right))) - (m_b^2 \\
& - 4q^2)\log\left(\frac{s-q^2}{m_b^2}\right)) - 2(10m_b^6(2q^2+s) - 10m_b^4(3q^4+5q^2s+s^2) + q^2(3q^6-23q^4s-3q^2s^2-7s^3) \\
& + m_b^2(11q^6+51q^4s+25q^2s^2+3s^3))\log\left(\frac{s}{m_b^2}-1\right)) + 6(-6(q^2-s)^3s(m_b^2+q^2+s)\log\left(\frac{s}{m_b^2}\right)^2 \\
& + 6(q^2-s)^3\log\left(\frac{m_b^2-s}{q^2-s}\right)(-(m_b^2(q^2+2s)) + s(m_b^2+q^2+s)\log\left(\frac{s-q^2}{m_b^2}\right)) + 3(q^2-s)^3s((m_b^2+q^2+s)
\end{aligned}$$

$$\begin{aligned}
& \times \log\left(\frac{m_b^2 - q^2}{s - q^2}\right)^2 - (m_b^2 + q^2 + s) \log\left(\frac{(m_b^2 - q^2)s}{m_b^2(s - q^2)}\right)^2 - 2(m_b^2 + q^2 + s) \log\left(\frac{(m_b^2 - q^2)s}{m_b^2(s - q^2)}\right) \log\left(\frac{s - q^2}{m_b^2}\right) \\
& + 2(2m_b^2 - 3q^2 + s) \log\left(\frac{s - q^2}{m_b^2}\right)^2 + 2 \log\left(\frac{m_b^2 - q^2}{s - q^2}\right) (-3m_b^2 + 6q^2 + (2m_b^2 - 3q^2 + s) \log\left(\frac{s - q^2}{m_b^2}\right)) \\
& + 2(m_b^8(-120q^2 + 170s) + 20m_b^6(9q^4 + 24q^2s - 10s^2) - 6m_b^4(12q^6 + 148q^4s + 123q^2s^2 - 3s^3) \\
& - 2q^2s(3q^6 + 98q^4s + 195q^2s^2 + 9s^3) + 2m_b^2q^2(3q^6 + 140q^4s + 531q^2s^2 + 216s^3) + 3s(s - q^2)^3 \\
& \times (5m_b^2 - 5q^2 + 3s) \log\left(\frac{s - q^2}{m_b^2}\right) \log\left(\frac{s}{m_b^2} - 1\right) - 6s(10m_b^8 - 10m_b^6(4q^2 + 3s) + 2s(q^2 + s) \\
& \times (11q^4 - 2q^2s + s^2) + 10m_b^4(5q^4 + 8q^2s + 2s^2) - m_b^2(23q^6 + 65q^4s + 41q^2s^2 + s^3)) \log\left(\frac{s}{m_b^2} - 1\right)^2 \\
& + \log\left(\frac{s}{m_b^2}\right) (-6m_b^2q^8 + q^4(120m_b^4 - 157m_b^2q^2 + 9q^4)s + (60m_b^6 + 60m_b^4q^2 - 243m_b^2q^4 + 205q^6)s^2 \\
& - 3(10m_b^4 + 43m_b^2q^2 - 121q^4)s^3 + 3(5m_b^2 + q^2)s^4 - 6(q^2 - s)^3s(m_b^2 + q^2 + s) \log\left(\frac{m_b^2 - q^2}{s - q^2}\right) \\
& - \log\left(\frac{(m_b^2 - q^2)s}{m_b^2(s - q^2)}\right) - \log\left(\frac{s - q^2}{m_b^2}\right) + 6s(q^8 + 24q^6s + 30q^4s^2 + 4q^2s^3 + s^4 - 20m_b^6(2q^2 + s) \\
& + 20m_b^4(3q^4 + 5q^2s + s^2) - m_b^2(25q^6 + 93q^4s + 59q^2s^2 + 3s^3)) \log\left(\frac{s}{m_b^2} - 1\right)) + 36s((-10m_b^8 \\
& + 10m_b^6s + 10m_b^4q^2(q^2 + 2s) + 4q^2s(q^4 + 3q^2s + s^2) - m_b^2(3q^6 + 25q^4s + 21q^2s^2 + s^3)) \text{Li}_2(1 - \frac{q^2}{m_b^2}) \\
& - (m_b^2 - 4q^2)(q^2 - s)^3(2\text{Li}_2(\frac{m_b^2 - s}{m_b^2 - q^2}) + \text{Li}_2(\frac{m_b^2 - s}{q^2 - s}) - \text{Li}_2(\frac{q^2(m_b^2 - s)}{m_b^2(q^2 - s)})) - (10m_b^8 - 5q^8 - 16q^6s \\
& - 54q^4s^2 - 4q^2s^3 - s^4 + 10m_b^6(4q^2 + s) - 10m_b^4(7q^4 + 12q^2s + 2s^2) + m_b^2(29q^6 + 115q^4s + 83q^2s^2 \\
& + 3s^3)) \text{Li}_2(1 - \frac{s}{m_b^2}))\} \\
\rho_{\text{T}4}^{2p} &= \frac{f_\pi m_b \mu_\pi^2}{120(q^2 - s)^7} (27a_2(2880m_b^{10} - 25m_b^8(215q^2 + 229s) + 20m_b^6(149q^4 + 447q^2s + 184s^2) \\
& - 10m_b^4(38q^6 + 352q^4s + 427q^2s^2 + 83s^3) + 5q^2(q^8 + 17q^6s + 42q^4s^2 + 22q^2s^3 + 2s^4) \\
& + m_b^2(-76q^8 + 84q^6s + 584q^4s^2 + 584q^2s^3 + 24s^4)) + 5(16128\eta_3m_b^{10}\omega_3 - 2520\eta_3m_b^8(15q^2 \\
& + 13s)\omega_3 + 8q^2((3 + 90\eta_3 + 10\eta_4)(q^2 - s)^2(q^4 + 5q^2s + 2s^2) - 9\eta_3(q^8 + 17q^6s + 42q^4s^2
\end{aligned}$$

$$\begin{aligned}
& +22 q^2 s^3 + 2 s^4) \omega_3) + 3 m_b^2 (20 q^4 s^2 (3 - 16 \eta_4 + 144 (\eta_3 + 2 \eta_3 \omega_3)) + q^6 s (69 + 320 \eta_4 + 240 \eta_3 (6 + 19 \omega_3) \\
& - 420 \eta_4 \omega_4) + 3 q^2 s^3 (-9 + 240 \eta_3 (-2 + 3 \omega_3) - 140 \eta_4 \omega_4) + 5 q^8 (-15 - 16 \eta_4 + 144 \eta_3 (-3 + \omega_3) + 84 \eta_4 \omega_4) \\
& + s^4 (-27 + 80 \eta_4 + 240 \eta_3 (-3 + \omega_3) + 420 \eta_4 \omega_4)) + 5 m_b^6 (s^2 (-33 + 352 \eta_4 + 144 \eta_3 (-8 + 33 \omega_3) + 756 \eta_4 \omega_4) \\
& + q^4 (-33 + 352 \eta_4 + 144 \eta_3 (-8 + 47 \omega_3) + 756 \eta_4 \omega_4) + 2 q^2 s (33 + 576 \eta_3 (2 + 11 \omega_3) - 4 \eta_4 (88 + 189 \omega_4))) \\
& + 3 m_b^4 (-15 q^2 s^2 (1 + 48 (\eta_3 + 16 \eta_3 \omega_3) - 12 \eta_4 (4 + 7 \omega_4)) - 3 q^4 s (53 + 1680 (\eta_3 + 3 \eta_3 \omega_3) - 20 \eta_4 (4 + 21 \omega_4)) \\
& + q^6 (111 + 240 \eta_3 (15 - 19 \omega_3) - 20 \eta_4 (20 + 63 \omega_4)) + s^3 (240 \eta_3 (9 - 10 \omega_3) - 7 (-9 + 20 \eta_4 (4 + 9 \omega_4)))) \\
& + 1080 m_b^2 (m_b^2 - q^2) (m_b^2 - s) (2 m_b^2 - q^2 - s) (q^2 - s) (6 a_2 - 35 \eta_4 \omega_4) (-\log(\frac{m_b^2 - s}{q^2 - s}) + \log(\frac{m_b^2 - q^2}{s - q^2})) \\
\rho_{T4}^{3p} = & \frac{-f_\pi m_b \mu_\pi^2}{24 (q^2 - s)^6} (m_b^2 - q^2) (80 \eta_4 (q^2 - s) (-8 m_b^4 + q^4 - 3 q^2 s - 6 s^2 + m_b^2 (q^2 + 15 s)) + 27 a_2 (45 m_b^6 + q^6 - 4 q^4 s \\
& - 30 q^2 s^2 - 12 s^3 - 5 m_b^4 (7 q^2 + 20 s) + m_b^2 (q^4 + 68 q^2 s + 66 s^2))) \\
T4_c = & \frac{-f_\pi m_b^2 m_b \mu_\pi^2}{160 (m_b^2 - q^2)^2} e^{\frac{-m_b^2}{M^2}} (12 a_2 + 5 (-25 + 48 \eta_3 (-10 + \omega_3)))
\end{aligned}$$

## References

- [1] V.M. Belyaev, A. Khodjamirian and R. Rückl, Z. Phys. C **60** (1993) 349 [hep-ph/9305348];  
A. Khodjamirian *et al.*, Phys. Lett. B **410** (1997) 275 [hep-ph/9706303];  
E. Bagan, P. Ball and V.M. Braun, Phys. Lett. B **417** (1998) 154 [hep-ph/9709243];  
A. Khodjamirian *et al.*, Phys. Rev. D **62** 114002 (2000) [hep-ph/0001297].
- [2] P. Ball and V. M. Braun, Phys. Rev. D **58** (1998) 094016 [arXiv:hep-ph/9805422].
- [3] P. Ball, JHEP **9809** (1998) 005 [hep-ph/9802394].
- [4] P. Ball and R. Zwicky, JHEP **0110** (2001) 019 [arXiv:hep-ph/0110115].
- [5] V.M. Belyaev *et al.*, Phys. Rev. D **51** (1995) 6177 [hep-ph/9410280];  
A. Khodjamirian *et al.*, Phys. Lett. B **457** (1999) 245 [hep-ph/9903421].
- [6] P. Colangelo and A. Khodjamirian, hep-ph/0010175;  
A. Khodjamirian, hep-ph/0108205.
- [7] 2nd Workshop on the CKM Unitarity Triangle, Durham, England, Apr 2003. Proceedings published as eConf C0304052.
- [8] T. Onogi, Talk at 2nd Workshop on the CKM Unitarity Triangle, arXiv:hep-ph/0309225, and references therein.

- [9] H. Li, hep-ph/0103305, and references therein;  
M. Beneke *et al.*, Phys. Rev. Lett. **83** (1999) 1914 [hep-ph/9905312]; Nucl. Phys. B **606** (2001) 245 [hep-ph/0104110].
- [10] C.H. Davies, talk at UK BaBar meeting, Durham April 2004.
- [11] J. Shigemitsu *et al.*, Nucl. Phys. Proc. Suppl. **129-130** (2004) 331 [arXiv:hep-lat/0309039].
- [12] V. L. Chernyak and A. R. Zhitnitsky, JETP Lett. **25** (1977) 510 [Pisma Zh. Eksp. Teor. Fiz. **25** (1977) 544];  
Sov. J. Nucl. Phys. **31** (1980) 544 [Yad. Fiz. **31** (1980) 1053];  
A.V. Efremov and A.V. Radyushkin, Phys. Lett. B **94** (1980) 245; Theor. Math. Phys. **42** (1980) 97 [Teor. Mat. Fiz. **42** (1980) 147];  
G.P. Lepage and S.J. Brodsky, Phys. Lett. B **87** (1979) 359; Phys. Rev. D **22** (1980) 2157;  
V.L. Chernyak, A.R. Zhitnitsky and V.G. Serbo, JETP Lett. **26** (1977) 594 [Pisma Zh. Eksp. Teor. Fiz. **26** (1977) 760]; Sov. J. Nucl. Phys. **31** (1980) 552 [Yad. Fiz. **31** (1980) 1069].
- [13] C. W. Bauer *et al.*, Phys. Rev. D **63** (2001) 114020 [arXiv:hep-ph/0011336].
- [14] C.W. Bauer, D. Pirjol and I.W. Stewart, Phys. Rev. D **67** (2003) 071502 [arXiv:hep-ph/0211069].
- [15] M.A. Shifman, A.I. Vainshtein and V.I. Zakharov, Nucl. Phys. B **147** (1979) 385; ibd. **147** (1979) 448.
- [16] V. M. Braun and I. E. Filyanov, Z. Phys. C **44**, 157 (1989) [Sov. J. Nucl. Phys. **50**];  
P. Ball, JHEP **9901** (1999) 010 [hep-ph/9812375].
- [17] A. Szczepaniak, E. M. Henley and S. J. Brodsky, Phys. Lett. B **243** (1990) 287.
- [18] E. Braaten, Phys. Rev. D **28** (1983) 524.
- [19] A. S. Kronfeld, Nucl. Phys. Proc. Suppl. **129** (2004) 46 [arXiv:hep-lat/0310063].
- [20] For instance, T. M. Aliev and V. L. Eletsky, Sov. J. Nucl. Phys. **38** (1983) 936 [Yad. Fiz. **38** (1983) 1537];  
E. Bagan *et al.*, Phys. Lett. B **278** (1992) 457.
- [21] A. A. Penin and M. Steinhauser, Phys. Rev. D **65**, 054006 (2002) [arXiv:hep-ph/0108110];  
M. Jamin and B. O. Lange, Phys. Rev. D **65**, 056005 (2002) [arXiv:hep-ph/0108135].
- [22] V. L. Chernyak and A. R. Zhitnitsky, Phys. Rept. **112** (1984) 173.
- [23] V. M. Braun and I. E. Filyanov, Z. Phys. C **44** (1989) 157 [Sov. J. Nucl. Phys. **50** (1989) 511].
- [24] S. V. Mikhailov and A. V. Radyushkin, Phys. Rev. D **45** (1992) 1754.



- [25] A. P. Bakulev, S. V. Mikhailov and N. G. Stefanis, arXiv:hep-ph/0405062.
- [26] G. Martinelli and C. T. Sachrajda, Phys. Lett. B **190** (1987) 151;  
T. A. DeGrand and R. D. Loft, Phys. Rev. D **38** (1988) 954;  
D. Daniel, R. Gupta and D. G. Richards, Phys. Rev. D **43** (1991) 3715.
- [27] L. Del Debbio *et al.* [UKQCD collaboration], Nucl. Phys. Proc. Suppl. **83** (2000) 235 [arXiv:hep-lat/9909147];  
L. Del Debbio, M. Di Pierro and A. Dougall, Nucl. Phys. Proc. Suppl. **119** (2003) 416 [arXiv:hep-lat/0211037].
- [28] J. Bijnens and A. Khodjamirian, Eur. Phys. J. C **26** (2002) 67 [arXiv:hep-ph/0206252].
- [29] A. Khodjamirian, Eur. Phys. J. C **6** (1999) 477 [arXiv:hep-ph/9712451].
- [30] A. Schmedding and O. Yakovlev, Phys. Rev. D **62** (2000) 116002 [hep-ph/9905392].
- [31] A. P. Bakulev, S. V. Mikhailov and N. G. Stefanis, Phys. Rev. D **67** (2003) 074012 [arXiv:hep-ph/0212250]; Phys. Lett. B **578** (2004) 91 [arXiv:hep-ph/0303039].
- [32] V.M. Braun, A. Khodjamirian and M. Maul, Phys. Rev. D **61** (2000) 073004 [hep-ph/9907495].
- [33] P. Ball and M. Boglione, Phys. Rev. D **68** (2003) 094006 [arXiv:hep-ph/0307337].
- [34] J. Charles *et al.*, Phys. Rev. D **60** (1999) 014001 [arXiv:hep-ph/9812358].
- [35] D. Becirevic and A. B. Kaidalov, Phys. Lett. B **478** (2000) 417 [arXiv:hep-ph/9904490].
- [36] A. Abada *et al.*, JHEP **0402** (2004) 016 [arXiv:hep-lat/0310050].
- [37] A. Khodjamirian, AIP Conf. Proc. **602** (2001) 194 [arXiv:hep-ph/0108205].
- [38] D. Becirevic *et al.*, JHEP **0301** (2003) 009 [arXiv:hep-ph/0212177].
- [39] M. B. Voloshin, Sov. J. Nucl. Phys. **50** (1989) 105 [Yad. Fiz. **50** (1989) 166].
- [40] W. A. Bardeen, E. J. Eichten and C. T. Hill, Phys. Rev. D **68** (2003) 054024 [arXiv:hep-ph/0305049].
- [41] P. Ball, arXiv:hep-ph/0308249.
- [42] D. Becirevic, arXiv:hep-ph/0211340.